PEOPLE'S DEMOCRATIC REPUBLIC OF ALGERIA

MINISTRY OF HIGHER EDUCATION AND SCIENTIFIC RESEARCH

UNIVERSITY OF SAAD DAHLAB BLIDA 1

Faculty of Technology

Department of Water Sciences and Environment

MASTER'S THESIS

Sector: Hydraulics
Specialty: Hydraulic Resources

Theme

Spatial Modeling of Water Erosion and Sediment Transport Using Geographic Information Systems (GIS)

(Case of Boughezoul Watershed)

Presented by:

BENCHERIF Ayat El Isra

Jury composed of:

Dr. MERABTI AbdelaazizBLIDA 1 university	President
Dr. BOUZERIA HousseynBLIDA 1 university	Examiner
Dr.BENKACI SouhilaBLIDA 1 university	Supervisor

Academic Year: 2024/2025

ملخص

تستندُ هذه الدراسةُ إلى نهجٍ مكانيٍّ متكامل يجمع بين نظم المعلومات الجغرافيّة (GIS) ومعادلة فقد التربة الشاملة المُنقَّحة (RUSLE)لتقييم تعرية التربة ونقل الرواسب في حوض بوغزول الواقع ضمن البيئة شبه الجافة بالجزائر. جرى إعداد خرائط لعوامل RUSLE عامل المطر R ، عامل القابلية للتعرية K ، عامل الطول-الانحدار LS ، عامل الغطاء النباتي C، وعامل الممارسات الزراعية P باستخدام نموذج الارتفاع الرقمي (DEM) ، وبيانات الهطول المطري، ومعلومات الغطاء الأرضي من قاعدة ESA World Cover ، وبيانات التربة من قاعدة .FAO-DSMW ولتجاوز محدودية RUSLEفي تمثيل نقل الرواسب، تم تقدير نسبة إيصال الرواسب (SDR) بأساليب تجريبية، وأظهرت النتائج أنّ نحو 17 ٪ من الرواسب المنجرفة تصل إلى مصبّ الحوض. فضلًا عن ذلك، حُسبت مؤشرات مورفومترية وهيدرولوجية عدّة (SPI، TRI، CTI، SDI) لتعزيز التوصيف المكاني لعمليات التعرية. وقد جُمعت الطبقات الموضوعية عبر جبر الخرائط لإنتاج خريطة مركّبة لمخاطر التعرية، أظهرت تباينًا كبيرًا في فقد التربة يتراوح بين 0.213 و 186 طن/هكتار/سنة، مع تركز أعلى للمخاطر على المنحدرات الزراعية الشديدة الانحدار ذات الغطاء النباتي المتناثر. تساعد هذه الخريطة في تحديد المناطق الأكثر هشاشة لتكون أولوية في تنفيذ تدابير حفظ التربة، ما يجعلها أداة دعم قرار قيّمة للإدارة المستدامة للتربة في البيئات شبه الجافة.

الكلمات المفتاحية :تعرية التربة؛ نقل الرواسب؛RUSLE ؛ نسبة إيصال الرواسب؛ نظم المعلومات الجغرافية.

Abstract (English)

The present study employs an integrated spatial approach, combining Geographic Information Systems (GIS) and the Revised Universal Soil Loss Equation (RUSLE) to assess water erosion and sediment transport in the Boughezoul watershed, located in semi-arid Algeria. The RUSLE factors (R, K, LS, C, and P) were mapped using a Digital Elevation Model (DEM), rainfall data, land cover information (ESA WorldCover), and soil data (FAO-DSMW).The Sediment Delivery Ratio (SDR) was estimated using empirical methods to address RUSLE's limitations in modeling sediment transport. Results indicate that approximately 17% of the mobilized sediments reach the watershed outlet. In addition, several morphometric and hydrological indices (SPI, TRI, CTI, SDI) were calculated to enhance the spatial characterization of erosive processes.Thematic layers were integrated through raster algebra to generate a composite erosion risk map. This final map highlights a marked variability in soil loss, ranging from 0.213 to over 186 t/ha/year. It illustrates a higher concentration of erosion risk on agricultural slopes with steep gradients and sparse vegetation cover. The map helps identify the most vulnerable zones, which may serve as priority areas for the implementation of soil conservation measures. It serves as a valuable decision-support tool for sustainable soil management in semi-arid environments.

Key words: Soil erosion, Sediment transport, RUSLE, Sediment Delivery Ratio, GIS.

Résumé (Français)

Cette étude propose une approche spatiale intégrée combinant les systèmes d'information géographique (SIG) et l'équation universelle révisée des pertes en sol (RUSLE). L'objectif est d'évaluer l'érosion hydrique et le transport sédimentaire dans le bassin versant de Boughezoul (Algérie).Les facteurs de l'équation RUSLE (R, K, LS, C et P) ont été cartographiés à partir d'un modèle numérique de terrain (MNT), de précipitations, de données d'occupation du sol (ESA WorldCover) etpédologiques (FAO-DSMW).Le coefficient de livraison des sédiments (SDR) a été estimé à l'aide de méthodes empiriques afin de pallier les limites de la RUSLE concernant le transport sédimentaire. Les résultats ont montré qu'environ 17 % des sédiments mobilisés atteignent l'exutoire du bassin. En complément, plusieurs indices morphométriques et hydrologiques ont été calculés (SPI, TRI, CTI, SDI) pour affiner la caractérisation spatiale des processus érosifs. Les couches thématiques ont été intégrées par algèbre raster pour produire une carte composite du risque d'érosion. La carte finale met en évidence une variabilité marquée des pertes en sol, allant de 0,213 à plus de 186 t/ha/an. Elle révèle une concentration accrue du risque d'érosion sur les versants agricoles à forte pente, où la végétation est peu dense. Cette carte permet de localiser les zones les plus exposées à l'érosion, susceptibles de constituer des secteurs prioritaires pour la mise en œuvre de mesures de conservation des sols.Elle constitue un très bon outil d'aide à la prise de décision pour la gestion durable des sols en milieu semi-aride.

Mots-clés : Érosion des sols, Transport des sédiments, RUSLE, Coefficient de livraison SDR, SIG

Acknowledgement

*First and foremost, **I thank God Almighty**, the source of strength, wisdom, and perseverance. It is by His will and mercy that I was able to carry out and complete this work. May His guidance continue to illuminate my path.*

*I extend my sincere gratitude to **Madame S. BENKACI**, my supervisor, for her constant availability, scientific rigor, and valuable guidance. Her kindness and support throughout this thesis have been a true source of encouragement and confidence.*

*I also wish to thank **the members of the jury** for taking the time to evaluate my work and for their constructive feedback, which will undoubtedly contribute to its improvement and my academic growth.*

*Finally, my deepest appreciation goes to **my dear parents**, whose unconditional love, silent sacrifices, and unwavering moral support have been my greatest source of strength. May this humble work be a reflection of their dedication and a source of pride.*

Dedication and Thanks

To my beloved parents, ***Brahim and Rachida****,*
whose unconditional love, tireless support, and endless sacrifices have shaped every step of my journey — this work is above all, yours.

To my dear brothers, ***M'Hamed*** *and* ***Aboubakre****,*
thank you for your strength, your encouragement, and for always standing beside me with pride and belief.

To my wonderful sisters, ***Salsabil****,* ***Sara****, and* ***Asma****,*
your love, support, and constant motivation have been a source of joy and inspiration throughout this path.

To my precious nieces and nephew, ***Ayoub****,* ***Lylia****,*
Hayat*,* ***Lina****, and* ***Loujaina****,*
your innocence, laughter, and smiles brought me light even in the most stressful days.

And to my fiancé, ***Mohamed****,*
Your quiet support and constant encouragement meant more than words can say.*This accomplishment is as much yours as it is mine.*

"With all my heart — thank you"

Table of Contents

List of Figures

List of Tables

Abbreviations

AI	Artificial Intelligence
A	Average Annual Soil Loss
DEM	Digital Elevation Model
DSMW	Digital Soil Map of the World
ESA	European Space Agency
FAO	Food and Agriculture Organization
GIS	Geographic Information System
IC	Index of Sediment Connectivity
LSTM	Long Short-Term Memory
LS	Slope Length and Steepness Factor
MODIS	Moderate Resolution Imaging Spectroradiometer
NDVI	Normalized Difference Vegetation Index
RS	Remote Sensing
RUSLE	Revised Universal Soil Loss Equation
SDR	Sediment Delivery Ratio
SRTM	Shuttle Radar Topography Mission
SY	Sediment Yield
TWI	Topographic Wetness Index
USDA	United States Department of Agriculture
UTM	Universal Transverse Mercator
WGS84	World Geodetic System 1984
SPI	Stream Power Index
TRI	Terrain Ruggedness Index
CTI	Compound Topographic Index
SDI	Sediment Deposition Index
LS	Slope Length and Steepness Factor
R	Rainfall Erosivity Factor
K	Soil Erodibility Factor
C	Cover-Management Factor
P	Support Practice Factor
IC	Index of Sediment Connectivity
KG	Gravelius Index
T/ha/yr	Tons per hectare per year
IDW	Inverse Distance Weighting
MAR	Mean Annual Rainfall

General Introduction

General Introduction

Soil erosion is defined as the detachment and movement of soil particles caused by agents such as water, wind, or tillage (Morgan, 2005). It constitutes a critical global issue of land degradation with major consequences for food security, water quality, and ecological resilience (Jones et al., 2019). In semi-arid and Mediterranean climates, exemplified by the northern regions of Algeria, the phenomenon is exacerbated by erratic, high-intensity rainfall, fragile soil compositions, sparse vegetative cover, and unsustainable anthropogenic land-use practices (Lal, 2001). The Boughezoul watershed represents a critical case where accelerated erosion significantly undermines agricultural productivity and contributes to the siltation of downstream hydraulic infrastructure. However, specific quantitative evidence on erosion severity in the region remains underreported, necessitating more localized studies.

Recent advances in erosion science have introduced dynamic modeling approaches integrating Geographic Information Systems (GIS), artificial intelligence (AI), and remote sensing technologies to improve the prediction of erosion under conditions where data is limited (Filchev& Kolev, 2023).Historically, the assessment of soil erosion has been based on empirical field measurements or point-scale runoff plots. Despite the high precision offered by these methods, their applicability at the watershed scale is limited due to logistical, temporal, and financial constraints. Furthermore, the absence of spatial continuity in such measurements imposes limitations on their utilization in the context of comprehensive land management planning. The integration of Geographic Information Systems (GIS), remote sensing technologies, and spatial modeling techniques has transformed the field by enabling high-resolution, reproducible evaluations of erosion dynamics (de Vente &Poesen, 2005).

The Revised Universal Soil Loss Equation (RUSLE) is one of the most widely used models for estimating average annual soil loss from sheet and rill erosion, based on climatic, edaphic, topographic, vegetative, and land management parameters (Renard et al., 1997). However, its empirical and static design limits its ability to simulate complex erosion processes such as gully formation and sediment deposition (Boix-Fayos et al., 2007; Tadesse et al., 2022). RUSLE also assumes spatially uniform rainfall and land cover, an oversimplification that proves inadequate in heterogeneous environments.To address the limitations of RUSLE in representing sediment transport processes, the Sediment Delivery Ratio (SDR) serves as an empirical corrective parameter used to estimate the proportion of eroded material that is ultimately delivered to the watershed outlet(Williams & Berndt, 1977). Although SDR

improves the realism of sediment transport modeling, its empirical origin and sensitivity to spatial heterogeneity often lead to significant uncertainties in predictive accuracy (Van Oost et al., 2009). Recent advancements, such as dynamic SDR models that integrate slope connectivity and rainfall thresholds, have demonstrated enhanced performance (Zhang et al., 2023). Moreover, terrain-based indices namely the Stream Power Index (SPI), Terrain Ruggedness Index (TRI), Compound Topographic Index (CTI), Sediment Deposition Index (SDI), and drainage density provide valuable insights into spatial variability in runoff generation, sediment flux, and geomorphological susceptibility (Moore et al., 1991; Wilson & Gallant, 2000).

In this context, the present study develops an integrated spatial modeling framework for the Boughezoul watershed to explicitly link soil detachment and sediment delivery processes. The methodology initiates with the calibration of the RUSLE model, utilizing region-specific datasets including precipitation, soil characteristics derived from the FAO Digital Soil Map of the World (DSMW), and land cover classifications from the ESA WorldCover 2020 product. Although these datasets offer comprehensive spatial coverage, their resolution and representativeness must be critically evaluated against local ground truth. Sediment delivery estimates are subsequently refined using both area-weighted and slope-informed SDR approaches. To further enhance spatial interpretation, relevant topographic indices are computed and standardized. Model validation is conducted through either field-based measurements or spatial correlation analyses to ensure methodological robustness and predictive reliability.

The central hypothesis of this study is that integrating empirical erosion metrics with topographic and process-based analysis improves the spatial accuracy of erosion risk assessment in data-scarce semi-arid environments, such as the Boughezoul watershed. This integrative approach aims to overcome the limitations of empirical models by incorporating terrain features and sediment transport mechanisms. However, its effectiveness depends on the availability of detailed and reliable input data, which is not always assured in such regions. The final output consists of a composite erosion risk map, generated through raster algebra in ArcGIS 10.4. This map serves as a decision-support tool for guiding targeted soil and water conservation strategies. In line with recent applications in Mediterranean environments (Benrhouma et al., 2024; Alemu et al., 2025), the present study aims to generate actionable insights for mitigating soil degradation. Its primary objective is to identify erosion hotspots and assess the effectiveness of conservation strategies tailored to local environmental conditions. The research supports both regional and national watershed management agendas by delineating erosion-prone zones, promoting soil-conserving agricultural practices, and

informing the design of sediment control infrastructure. However, the generalisability of the proposed approach must be evaluated cautiously, as variations in hydrological regimes, land use, and data availability may affect its broader applicability. Although the framework is methodologically robust, site-specific calibration may still be necessary to ensure successful transferability.

This thesis is organized into four main chapters. Chapter 1 provides comprehensive literature review covering soil erosion processes, modeling approaches, and the use of GIS and remote sensing in erosion assessment. Chapter 2 describes the physical, climatic, geological, and land use characteristics of the Boughezoul watershed. Chapter 3 outlines the data sources, methodological framework, and GIS-based techniques used for estimating soil loss and sediment yield. Chapter 4 presents and discusses the results, including erosion factor maps, sediment yield estimation, terrain–hydrologic indices, and the final erosion risk map, along with implications for watershed management.

Chapter 1

Literature Review

Chapter 1 Literature Review

1.1 Overview of Soil Erosion

Soil erosion is a complex, multidimensional geomorphological process involving the detachment, transport, and deposition of soil particles. It is primarily driven by hydrological and aeolian forces. Although it is a natural component of landscape evolution, human activity has significantly intensified its impacts. Land mismanagement, deforestation, and unsustainable agricultural practices have exacerbated erosion to the point where it is now a major global environmental concern, with increasingly severe consequences. These include reduced agricultural productivity, reservoir sedimentation, biodiversity loss, and degraded water quality (Andualem, 2013).

The Sediment Delivery Ratio (SDR) quantifies the proportion of eroded soil that ultimately reaches the outlet of a watershed or a defined stream location. This metric accounts for intermediate deposition influenced by terrain roughness, vegetative barriers, and conservation structures (Renard et al., 1997). Accurate SDR estimation is essential for converting gross soil loss into actual sediment yield, a key variable in infrastructure design, land-use planning, and ecological impact assessments.

Soil erosion caused by water generally occurs in four main forms:

• Splash erosion: when raindrops dislodge soil particles upon impact;
• Sheet erosion: the uniform removal of topsoil by shallow overland flow;
• Rill erosion: characterized by the formation of small channels as runoff becomes more concentrated;
• Gully erosion: involving deeper cuts formed by fast-moving water during heavy storms (Mitasova et al., 2013).

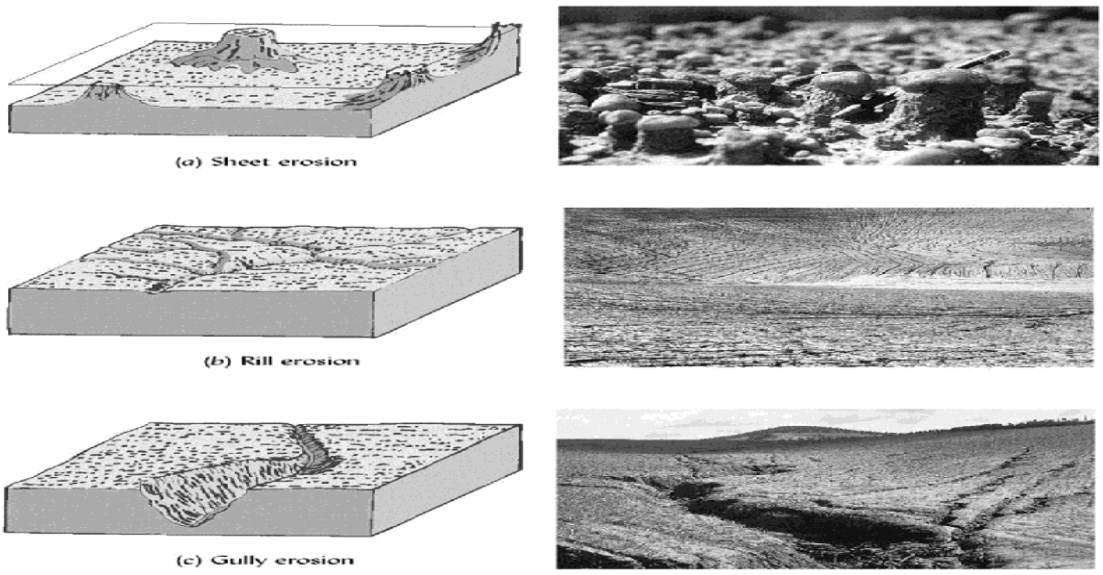

Figure 1.1: Sheet,Rill,Gully progression (Rojak, 2019)

SDR acts as a crucial link between erosion models such as RUSLE and measured sediment yield, making it indispensable for real-world applications. However, traditional approaches, such as the USDA SDR equation, which is primarily based on catchment area (Vanoni, 1975), often fail to capture the spatial and temporal complexity of natural systems.

To address these limitations, recent studies have explored more dynamic approaches. For example, incorporating sediment connectivity on hill slopes and thresholds related to rainfall intensity has improved SDR predictions on both monthly and event scales (Borselli et al., 2008; Brooks & Spencer, 2019; de Vente et al., 2023). These models recognize that not all eroded material is equally mobile or reaches the catchment outlet, depending on terrain complexity, vegetation, and deposition zones. Studies also show that incorporating region-specific factors, such as adaptive land cover coefficients or rainfall-driven transport responses, enhances the ability to capture spatial and temporal SDR variability (Zhang et al., 2010). Moreover, understanding the hydraulic behavior of sediment-laden flows during storm events offers insights into intermediate deposition patterns and helps refine SDR estimation (Loch et al., 2001). Altogether, these dynamic frameworks offer a more robust and context-sensitive basis for predicting sediment transport across diverse environmental and climatic settings.

1.1.1 Erosion Drivers and Sediment Transport Dynamics

The extent and severity of soil erosion result from the interaction of climatic, topographic, edaphic, and anthropogenic factors. Intense precipitation increases the kinetic energy of raindrops and surface runoff, accelerating the detachment and transport of soil particles. Soil

texture, structure, organic matter content, and permeability all influence erodibility, with coarser and poorly aggregated soils being particularly vulnerable. Steeper slopes enhance runoff velocity, while limited vegetative cover reduces resistance to raindrop impact and flow concentration. Anthropogenic drivers such as deforestation, overgrazing, intensive agriculture, and urban expansion further exacerbate erosion processes. These human-induced disturbances remove protective vegetation, degrade soil structure, and often increase runoff coefficients (Panagos et al., 2015).

Recent advancements have led to high-resolution, GIS-based approaches for improving SDR estimation across heterogeneous landscapes. These approaches incorporate terrain-sensitive metrics such as slope, flow accumulation, drainage density, and land use classification. Notably, the Index of Sediment Connectivity (IC), developed byBorselli et al. (2008), integrates upslope and downslope conditions to quantify sediment transfer potential at sub-watershed scales. It has proven especially effective in Mediterranean and semi-arid environments.

Sediment transport mechanisms are generally categorized as either suspended load or bedload. Fine particles remain suspended in the water column, while coarser materials are transported by rolling, sliding, or saltation along the streambed. Sediment transport capacity is primarily governed by stream discharge, slope gradient, and channel morphology. Storm events and seasonal floods often cause sharp increases in sediment fluxes, leading to downstream sedimentation in reservoirs and alluvial plains. This process reduces storage capacity and degrades aquatic habitats (Panagos et al., 2015).

In the Boughezoul watershed, implementing a simplified, catchment-scale SDR model integrated with RUSLE-derived gross erosion estimates has proven both feasible and effective. This combined approach helps identify sediment source hotspots and supports spatially optimized, cost-efficient land management strategies (Borrelli et al., 2021).A mechanistic understanding of erosion drivers and sediment routing is essential for designing resilient conservation practices and informing watershed-scale decision-making, especially in environmentally vulnerable regions like Boughezoul.

1.1.2 Modeling Soil Erosion and Sediment Transport

Modeling soil erosion and sediment transport is essential for predicting soil loss and guiding sustainable land management strategies. These models are generally categorized as empirical, conceptual, or physically based, each with varying degrees of complexity, data requirements, and spatial resolution (Mitasova et al., 2013).

The Revised Universal Soil Loss Equation (RUSLE) remains one of the most widely applied empirical models for estimating long-term average annual soil loss. It integrates multiple biophysical factors: rainfall erosivity (R), soil erodibility (K), topographic influence (LS), vegetation cover and management (C), and support practices (P). RUSLE's simplicity, adaptability, and compatibility with Geographic Information Systems (GIS) make it especially useful for large-scale assessments (Ganasri& Ramesh, 2016). Although RUSLE is empirical in nature, its integration with GIS platforms enables spatially explicit identification of erosion-prone zones, supporting both scenario-based simulations and targeted interventions. The model has demonstrated effectiveness in a wide range of environmental settings, including Mediterranean and semi-arid regions.

In the context of the Boughezoul watershed, RUSLE offers a practical and robust modeling framework. Its modest input data requirements are particularly advantageous in data-scarce environments. When calibrated with global datasets such as ESA WorldCover and FAO DSMW, its applicability is further enhanced. Combined with Sediment Delivery Ratio (SDR) models, RUSLE becomes a powerful tool for estimating sediment yield and for prioritizing zones for conservation (Benavidez et al., 2018).While RUSLE does not explicitly simulate dynamic erosion processes such as gully formation or sediment deposition, its overall flexibility and performance justify its selection in this study. When coupled with terrain analysis and remote sensing inputs, it offers reliable spatial representation of erosion risk (Alewell et al., 2019).

1.1.3 Integration of GIS in Erosion and Sediment Modeling

The integration of Geographic Information Systems (GIS) into erosion modeling has significantly advanced soil conservation analysis by introducing spatial precision, automation, and analytical scalability. GIS allows for the collection, processing, and visualization of geospatial datasuch as slope gradients, land cover, soil types, and rainfall distribution which are key variables in erosion risk assessment and sediment yield modeling (Mitasova et al., 2013).

In modeling frameworks such as RUSLE, GIS facilitates the generation of spatial layers for each model factor: Digital Elevation Models (DEMs) provide slope and flow direction for the LS factor; land cover maps are used to derive the C factor; soil databases define the K factor; and rainfall data are used to calculate the R factor. These layers are integrated using raster algebra techniques to produce detailed, spatially explicit erosion risk maps (Ganasri&Ramesh,

2016). GIS-based erosion modeling is especially valuable in regions with limited field data. The integration of global datasets such as ESA WorldCover, SRTM, and FAO DSMW, with locally calibrated parameters enables cost-effective, large-scale erosion assessments (Benavidez et al., 2018). GIS also supports scenario based analyses, such as simulating the effects of land use change, conservation measures, and climate variability on erosion dynamics.

In the Boughezoul watershed, GIS plays a central role in mapping erosion hotspots and prioritizing sub-watersheds for intervention. The incorporation of topographic indices such as the Stream Power Index (SPI), Topographic Wetness Index (TWI), and the Index of Sediment Connectivity (IC), enhances model accuracy by capturing sediment transport potential and spatial variability (Borselli et al., 2008; Cavalli et al., 2013).Ultimately, GIS improves the reliability of erosion modeling outputs and supports participatory watershed planning by providing clear visualizations that inform decision-making, policy development, and resource allocation.

1.2 Erosion Modeling Approaches

1.2.1 Empirical vs. Physically-Based Models

Erosion models are commonly categorized into two major types: empirical and physically based frameworks, each with distinct methodological foundations and data requirements. Empirical models rely on observed data and statistical relationships to estimate average soil loss. These models such as RUSLE are particularly well suited for large-scale or data limited environments due to their simplicity, ease of implementation, and compatibility with GIS platforms (Panagos et al., 2015). In contrast, physically based models simulate the underlying hydrological and geomorphologic processes that govern erosion. They account for rainfall-runoff generation, sediment detachment, transport, and deposition by solving complex equations typically partial differential equations. These models require high-resolution input data, such as rainfall intensity, infiltration rates, soil cohesion, and vegetation dynamics, to achieve reliable outputs (Epple et al., 2022). While physically based models offer a more detailed and mechanistic understanding of erosion dynamics, their real-world application is often limited by data scarcity, high computational demands, and complex calibration procedures particularly in semi-arid and data-constrained regions.

Given the limited hydro meteorological data available in the Boughezoul watershed and the need for spatial prioritization of interventions, an empirical approach specifically, the use of

RUSLE was selected. This choice offers a balance between practicality and spatial accuracy, enabling the identification of erosion-prone zones and supporting land-use planning efforts (Ganasri& Ramesh, 2016).

1.2.2 The Revised Universal Soil Loss Equation (RUSLE)

The Revised Universal Soil Loss Equation (RUSLE) is a widely used empirical model designed to estimate long-term average annual soil loss caused by sheet and rill erosion. Developed as an enhancement of the original USLE framework, RUSLE includes updated equations and parameterizations to accommodate a broader range of land management practices and environmental conditions (Renard et al., 1997).

RUSLE is expressed as follows:

$$A = R \times K \times LS \times C \times P \quad \ldots\ldots\ldots\ldots\ldots\ldots\ldots\ldots\ldots\ldots\ldots\ldots \quad (1)$$

Where:

A: estimated average annual soil loss (tons/ha/year)

R: rainfall erosivity factor (reflects raindrop impact energy and storm frequency)

K: soil erodibility factor (represents the soil's susceptibility to detachment)

LS: slope length and steepness factor (topographic control on runoff velocity and volume)

C: cover-management factor (influence of vegetation, crop type, and land use)

P: support practice factor (effectiveness of conservation practices such as terracing or contour farming).

Each factor can be derived from geospatial and remote sensing datasets, allowing for spatially continuous erosion mapping. RUSLE's compatibility with GIS platforms makes it highly effective for watershed-scale planning and erosion control design (Benavidez et al., 2018). The R-factor is typically calculated from long-term rainfall data, either interpolated from meteorological stations or extracted from satellite-based precipitation products. The K-factor is commonly sourced from global soil databases such as FAO's Digital Soil Map of the World (DSMW). The LS-factor is derived from high-resolution Digital Elevation Models (DEMs), while C and factors are estimated using classified land cover datasets (e.g., ESA WorldCover) and field- or expert-based assessments of local conservation practices.

RUSLE's strength lies in its simplicity, robust validation history, and adaptability to global datasets. In the Boughezoul watershed, where field measurements are scarce and spatial variability is high, RUSLE enables the identification of high-risk zones and supports

evidence-based land use planning. Furthermore, when integrated with Sediment Delivery Ratio (SDR) models, RUSLE provides a comprehensive framework for estimating sediment yield at the watershed outlet. This combined approach has proven effective in erosion assessment and management across Mediterranean and semi-arid regions (Alewell et al., 2019).

1.2.3 Sediment Delivery Ratio (SDR) Estimation Models

The Sediment Delivery Ratio (SDR) represents the proportion of eroded soil that is ultimately delivered to a watershed outlet, thus bridging the gap between gross soil loss estimates and actual sediment yield. SDR accounts for intermediate deposition processes that occur as sediment is transported, influenced by terrain configuration, vegetation cover, and land use practices (de Vente et al., 2023). Traditionally, SDR has been estimated using empirical relationships most notably the USDA formula, which expresses SDR as a function of watershed drainage area (Vanoni, 1975). Although simple and widely applied, such methods often oversimplify the complexity of terrain and lack spatial precision.

Recent advancements have led to the development of GIS-based, spatially explicit SDR models that incorporate variables such as slope gradient, flow length, drainage density, land use, and vegetation cover. These factors are essential for assessing sediment connectivity across landscapes. One major innovation is the Index of Sediment Connectivity (IC), proposed by Borselli et al. (2008), which quantifies sediment transfer potential by integrating upslope contributing area with downslope flow pathways. This index has been validated in both Mediterranean and semi-arid environments.

In data-limited regions such as the Boughezoul watershed, integrating SDR with RUSLE derived gross erosion estimates enables a practical and cost-effective means of estimating sediment yield. This approach supports the prioritization of sub-watersheds for intervention and improves the spatial targeting of soil conservation efforts (Borrelli et al., 2021). Incorporating SDR into erosion modeling is essential for effective watershed management. It informs decisions related to reservoir sedimentation, infrastructure maintenance, and investment in erosion control strategies. Moreover, SDR modeling enhances the alignment between modeled predictions and observed sediment deposition patterns, contributing to more accurate, field relevant outcomes.

1.3 GIS and Remote Sensing Applications in Soil Erosion Modeling

Geographic Information Systems (GIS) and Remote Sensing (RS) technologies have revolutionized soil erosion assessment by enabling spatial data integration, advanced analysis, and effective visualization. When combined with empirical models such as RUSLE, these tools support high-resolution, spatially explicit erosion risk mapping even in regions with limited ground-based data (Mitasova et al., 2013).GIS forms the analytical backbone of erosion modeling, allowing for the creation, manipulation, and management of key spatial layers. For instance, Digital Elevation Models (DEMs) are used to compute slope gradient and slope length (LS factor), while land use/land covers mapsinform the cover-management factor (C). Soil property datasets help estimate the soil erodibility factor (K), and vector-based datasets can be used to define support practices (P). GIS terrain analysis tools also compute flow direction, drainage networks, and hydrological connectivity, which enhance model accuracy (Ganasri& Ramesh, 2016).

Remote Sensing provides near-real-time, scalable access to environmental variables such as vegetation indices (e.g., NDVI), land cover change, and soil moisture. Satellite platforms like Sentinel-2**,** Landsat**,** andMODIS enable the dynamic updating of RUSLE input layers, particularly for C and K factors. These RS products are essential for capturing seasonal variations in erosion susceptibility (Singh & Mishra, 2014). The integration of RS data within GIS environments improves the spatial and temporal precision of erosion modeling. It reduces the reliance on costly and time-consuming field measurements and supports multi-temporal analysis, scenario simulation (e.g., land use change), and evidence-based decision-making.

In the Boughezoul watershed**,** the combined use of GIS and RS is especially valuable due to its rugged terrain and limited in-situ monitoring infrastructure. By leveraging global datasets and satellite imagery, erosion risk maps can be developed to guide conservation priorities and inform sustainable land and water management strategies (Alewell et al., 2019).

1.4 Terrain and Hydrological Indices in Erosion Analysis

Terrain and hydrological indices provide critical insight into the spatial variability of erosion and sediment transport by quantifying landform morphology, flow dynamics, and geomorphic sensitivity. These metrics are particularly useful for identifying areas prone to runoff concentration, sediment connectivity, and landform instability (Wilson & Gallant, 2000).The Stream Power Index (SPI) estimates the erosive force of surface runoff by combining slope gradient and upslope contributing area. High SPI values are typically associated with

concentrated flow paths such as rills, gullies, and stream channels making this index a strong predictor of erosion hotspots (Moore et al., 1991).

The Terrain Ruggedness Index (TRI) measures variation in elevation within a defined neighborhood. Areas with high TRI values often correspond to complex topography and increased soil detachment potential, especially during high-intensity rainfall events (Riley et al., 1999). The Compound Topographic Index (CTI)**,** also known as the Topographic Wetness Index (TWI)**,** estimates the spatial distribution of soil moisture based on upslope contributing area and slope. Zones with high CTI values are typically more saturated and subject to overland or shallow subsurface flow, influencing both erosion and deposition processes (Beven& Kirkby, 1979). The Slope Development Index (SDI) captures curvature in the terrain, distinguishing convex forms (erosion-prone) from concave forms (depositional). When analyzed alongside slope and aspect, SDI enhances spatial interpretations of runoff behavior and sediment dynamics (Ali et al., 2016). Drainage density**,** defined as the total length of stream channels per unit area, reflects the efficiency of runoff concentration and removal. High drainage density is often linked to higher erosion rates, especially in steep, sparsely vegetated areas (Gomi et al., 2002).Integrating these indices into GIS-based erosion models significantly improves the accuracy of erosion hotspot prediction. In the Boughezoul watershed**,** such terrain metrics help prioritize intervention zones and support the design of targeted, cost-effective soil and water conservation strategies.

1.5 Conclusion

Soil erosion is a complex process driven by both natural forces and human activities, with significant environmental and economic impacts. This chapter highlighted the role of the Sediment Delivery Ratio (SDR) in linking erosion to sediment yield, and reviewed the strengths and limitations of various modeling approaches.

Among them, RUSLE combined with GIS and Remote Sensing proves especially effective in data-scarce regions. The integration of terrain and hydrological indices further enhances model accuracy, allowing for better identification of erosion-prone areas and more informed conservation planning.

Chapter 2
Study Area

2 Chapter 2: Study Area

2.1 Natural and Physical Features of the Boughezoul Watershed

2.1.1 Geographic Context of the Boughezoul Watershed

The Boughezoul watershed is located in the north-central part of Algeria (Figure 2.1), within the semi-arid high plateaus of Médéa Province, approximately 130 km south of Algiers. It is part of the Chelif River Basin, one of the largest and most significant hydrological systems in the country. Spanning an area of approximately 350 to 400 km², the watershed includes a variety of land cover types, such as agricultural zones, rangelands, and sparsely vegetated areas. It is situated between latitudes 35°50′N and 36°10′N and longitudes 2°30′E and 3°00′E (ANRH, 2021). This region plays a crucial role in agricultural production and water resource management, particularly with the planned construction of the Boughezoul Dam, which is intended to support both irrigation and flood control. Land use is influenced by topography, climatic variability, and seasonal human activities, all of which contribute to soil degradation and increased surface runoff (Hamelin et al., 2020). Positioned between the Tellian Atlas and the Saharan fringe, the watershed exhibits a combination of Mediterranean and arid features, making it a representative case study for soil erosion in climate-sensitive environments (Benchetrit et al., 2018).

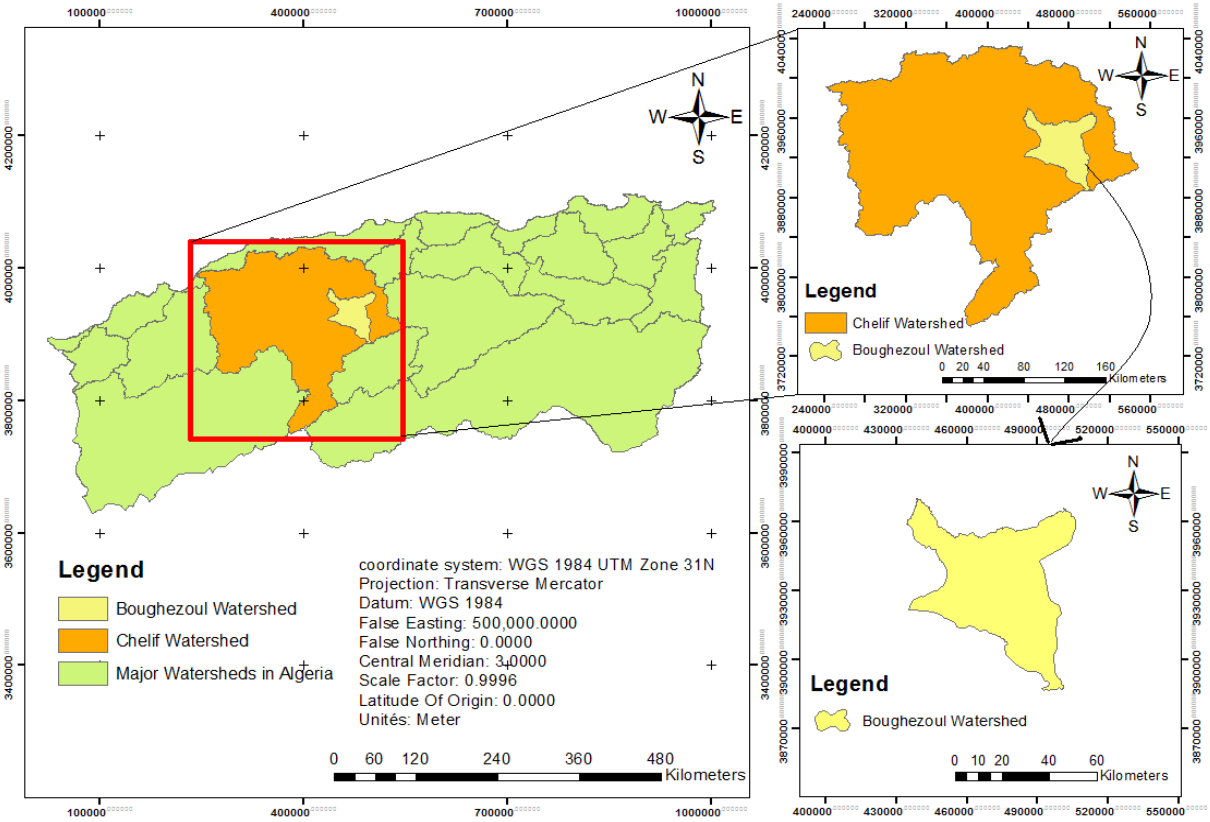

Figure 2.1: Geographic location of the Boughezoul Watershed (Algeria).

2.1.2 Topographic and Hypsometric Analysis

The topographic structure exerts a pivotal influence on the processes of erosion, runoff, and sediment dynamics in semi-arid watersheds. To characterize the altitudinal configuration of the Boughezoul watershed, a Digital Elevation Model (DEM) and a hypsometric map were generated using ASTER DEM data and processed in ArcGIS. These tools provide complementary insights into elevation distribution, slope gradient, and the stage of geomorphic evolution. The DEM (Figure 2.2) reveals an elevation range extending from approximately 620 meters in the southern plains to over 1,704 meters in the northern uplands. The northern and northeastern sectors exhibit rugged terrain with steep slopes, indicating higher runoff potential and pronounced erosion activity. In contrast, the southern and central parts of the basin are characterized by broader, flatter topography, which favors sediment deposition and infiltration.

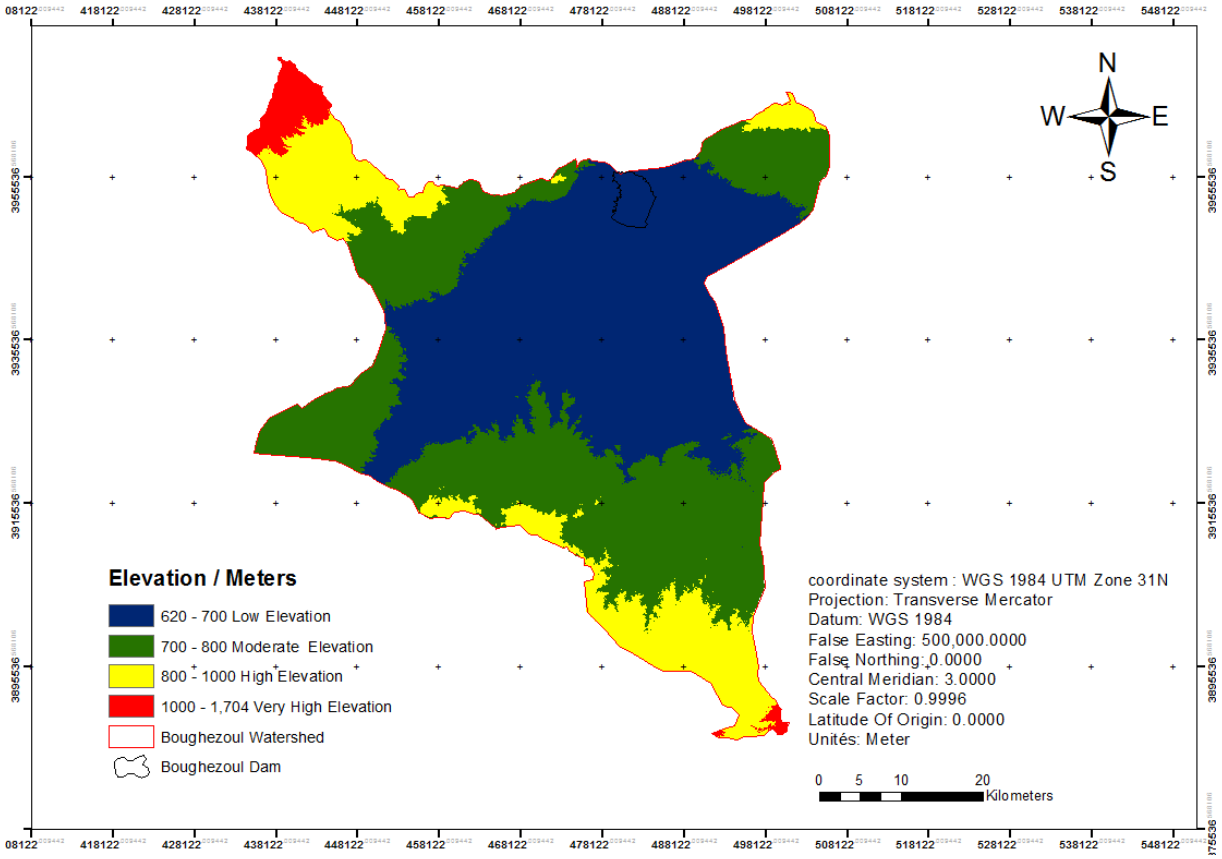

Figure 2.2: Digital Elevation Model (DEM) of the Boughezoul Watershed.

The hypsometric structure of the watershed was analyzed using elevation-class distribution extracted from the DEM. the hypsometric curve (Figure 2.3) shows the cumulative surface distribution with respect to elevation.

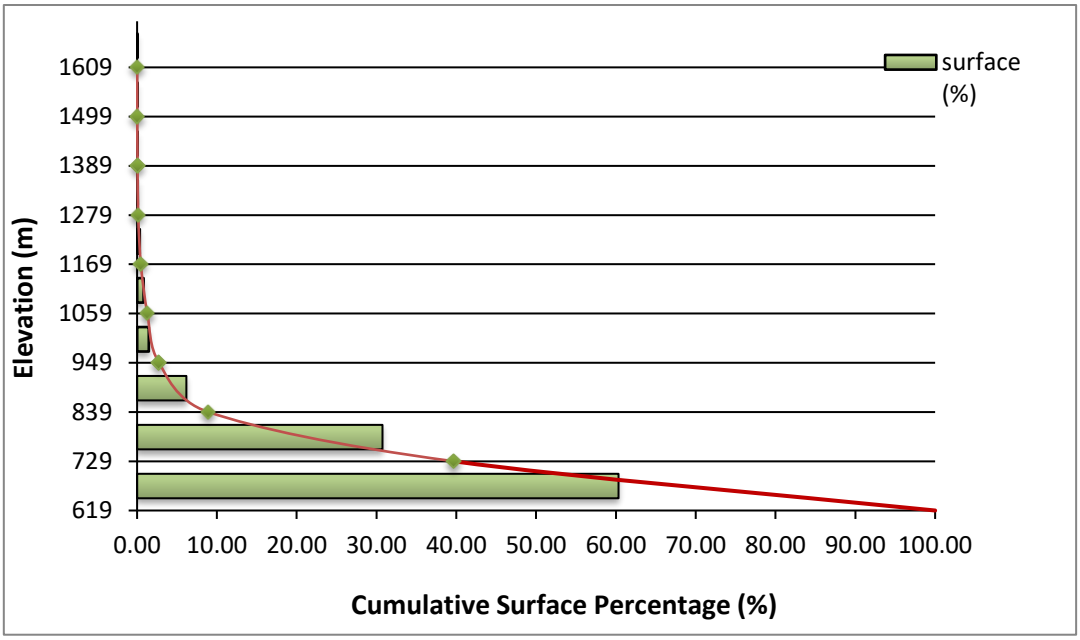

Figure 2.3: Hypsometric Curve of the Boughezoul Watershed.

This analysis confirms the watershed's mature geomorphic stage, with the majority of the terrain situated between 619 and 839 meters, representing transition zones between upland erosion sources and midstream deposition areas. To complement this analysis, a hypsometric map was generated (Figure 2.4), offering a spatial representation of the elevation class distribution across the watershed. This is particularly evident in the intermediate elevations (800–1,200 m), which encompass a significant portion of the watershed and function as transition zones between sediment sources and sinks.

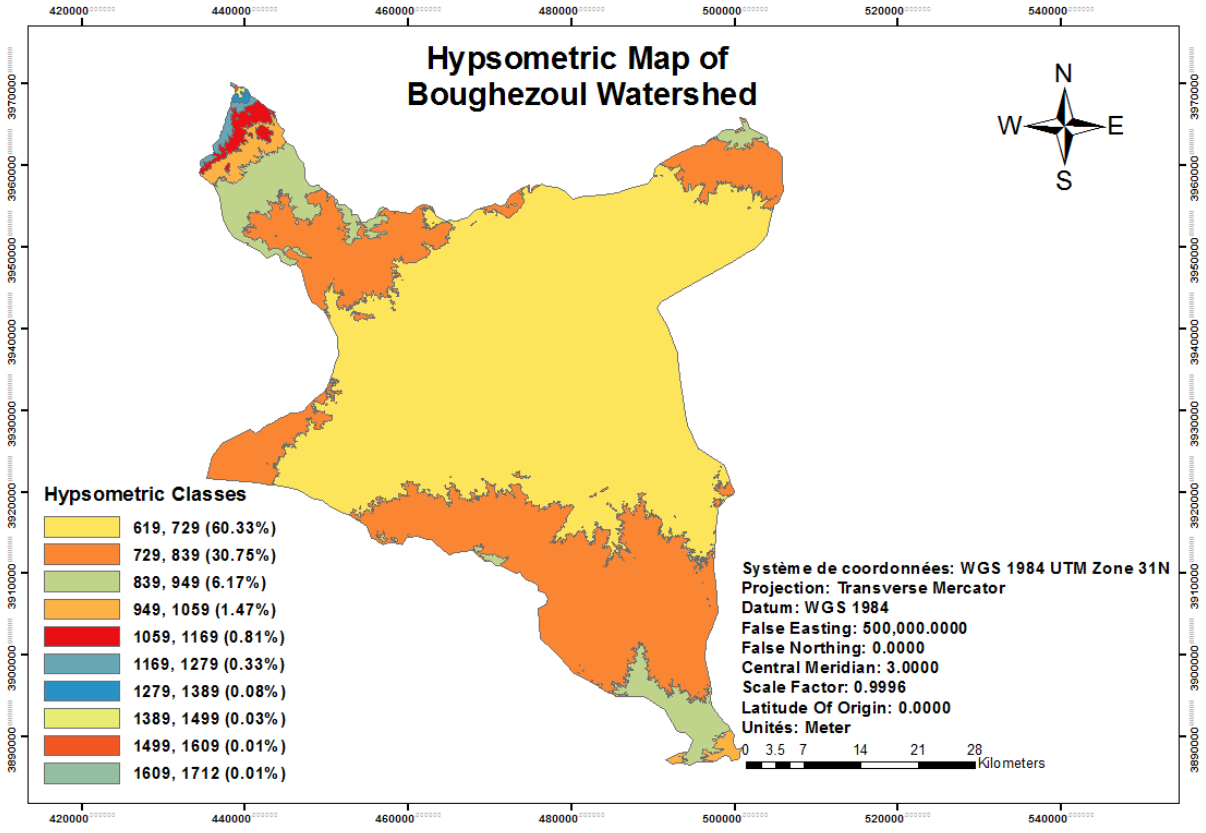

Figure 2.4: Hypsometric Map of the Boughezoul Watershed.

2.1.3 Geology

From a geological perspective, the Boughezoul watershed is primarily composed of Neogene to Quaternary sedimentary formations, including marl, clay, sandstone, and alluvial deposits. These materials are generally weakly consolidated, making them highly susceptible to erosion. In the northern regions, limestone and calcareous outcrops dominate, while lacustrine deposits are prevalent in the central areas. These geological substrates significantly influence soil texture, infiltration capacity, and land stability critical factors in assessing erosion risk (Belhadj et al., 2013; Fehdi et al., 2017). The geological map (Figure 2.5) illustrates the spatial distribution of sedimentary formations across the watershed, highlighting the predominance of marl, clay, sandstone, and alluvial deposits. These weakly consolidated lithologies are particularly vulnerable to erosion under surface flow conditions. In the northern sector, limestone and calcareous rocks are associated with steeper slopes, whereas the central basin is characterized by widespread lacustrine formations, often linked to reduced infiltration and increased runoff potential. The geological heterogeneity of the watershed largely accounts for the variability in erosion susceptibility and runoff behavior observed across the region.

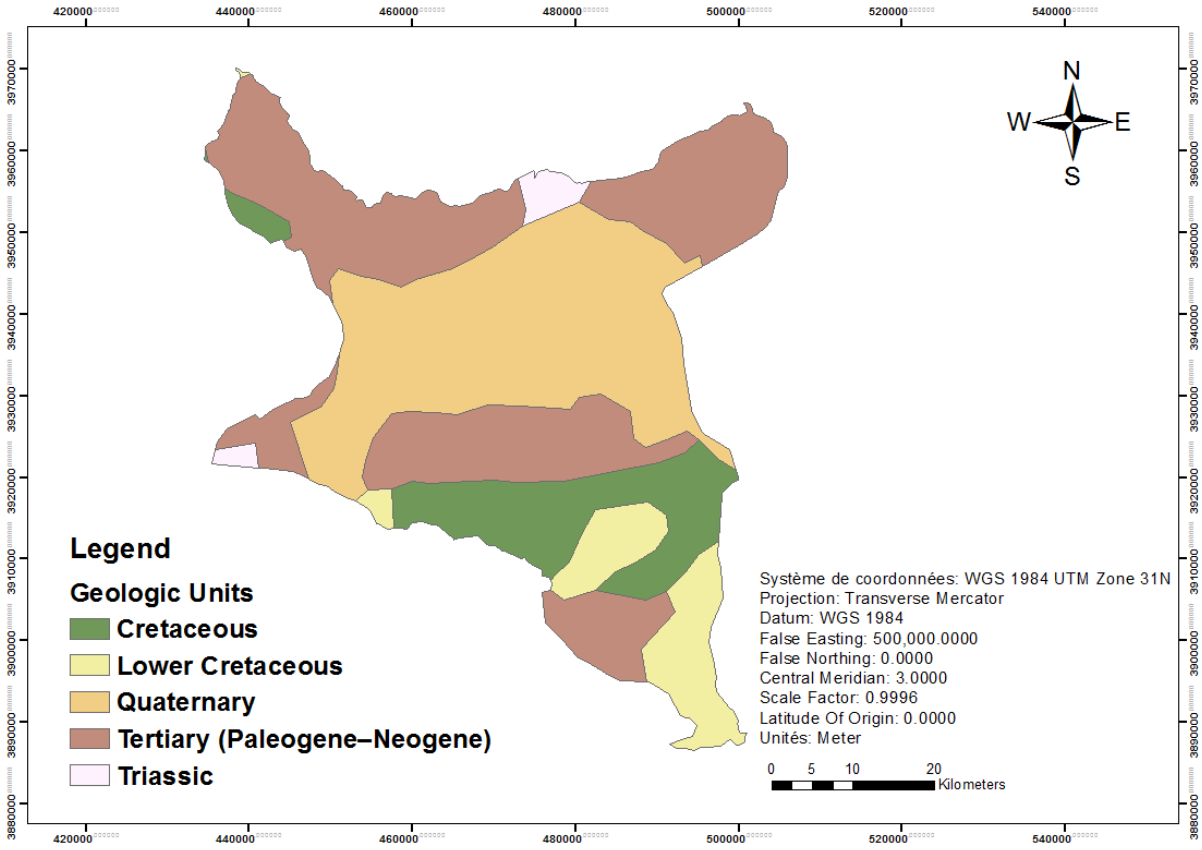

Figure 2.5: Geological Map of the Boughezoul Watershed.

Cretaceous: Limestone, marl, sandstone (marine sediments).

Lower Cretaceous: Clay-limestone, sandstone, sometimes marl.

Quaternary: Recent deposits: alluvium, colluviums, terraces.

Tertiary (Paleogene–Neogene): Clay, marls, conglomerates, possibly lacustrine.

Triassic: Evaporites, dolomites, red beds (older layers).

2.1.4 Climate and Hydrology

The Boughezoul watershed exhibits a semi-arid Mediterranean climate, characterized by hot, dry summers and mild, wet winters. Annual precipitation ranges from 300 to 450 mm, with considerable interannual variability. Rainfall predominantly occurs in autumn and winter, often in the form of brief but intense events, which generate significant surface runoff and contribute to soil erosion (Bessaoud et al., 2018). Temperatures typically vary between approximately 5°C during the winter and over 35°C in the summer, resulting in elevated evapotranspiration rates that promote soil crusting, particularly in regions with sparse vegetation cover (Nouiri et al., 2015). Hydrologically, the watershed is drained by the Boughezoul Wadi, a seasonal tributary of the Chelif River. Stream flow is ephemeral, with discharge exhibiting high variability and minimal base flow, thereby increasing the susceptibility to flash floods and sediment transport (Boudjemaa et al., 2021).

2.2 Soil Characteristics

The Boughezoul watershed features **a** heterogeneous soil profile shaped by the interplay of semi-arid climatic conditions**,** topographic variability**,** and underlying geological formations**.** The main soil types across the basin include Calcisols**,** Regosols**,** and Vertisols each exhibiting distinct morphological and hydrological characteristics that influence their erosion susceptibility **(FAO, 2020).** Calcisols dominate the gently sloping plains. These soils are characterized by high calcium carbonate accumulation, moderate structure, and low organic matter content. While relatively stable under natural vegetation, they are prone to surface sea ling and crust formation when disturbed or left bare, reducing infiltration and increasing runoff (Benabderrahmane et al., 2016). Regosols, typically found on steeper and degraded slopes**,** are shallow, poorly developed soils with limited cohesion and low water-holding capacity**.** These characteristics make them highly vulnerable to detachment, rillinitiation, and sediment transport, especially under intense rainfall (Hamza et al., 2015). Vertisols, occurring mainly in the southern parts of the watershed, are deep clayey soils with pronounced shrink swell behavior. Their high bulk density limits deep infiltration, and their tendency toward surface sealing on concave terrain can lead to concentrated runoff and localized erosion during heavy storms. Soil textures across the basin range from sandy loam to silty clay, contributing to considerable spatial variation in hydraulic behavior and erosion potential. Finer-textured soils, especially when unconsolidated, are more prone to overland flow and sediment generation during high-intensity precipitation events. In addition to natural factors, anthropogenic pressures such as intensive tillage, overgrazing, and vegetation removal exacerbate soil fragility. These practices disrupt aggregate stability, deplete organic matter, and compact the upper layers, further increasing erosion risk (Hadji et al., 2020).

Recent regional research (Mansouri et al., 2021**)** emphasizes the value of integrating high-resolution soil property datasets such as FAO DSMW and Soil Grids into erosion modeling frameworks. This enhances the ability to represent local variations in erodibility and supports the design of tailored soil conservation strategies**.**

2.3 Land Use and Human Impact

Land use in the Boughezoul watershed consists of a mosaic of agricultural fields, grazing lands, sparse shrublands**,** and dispersed urban infrastructure. The dominant land-use activity is rainfed cereal cultivation, primarily wheat and barley, while extensive livestock grazing occurs on marginal and degraded terrains. These practices, often carried out with minimal regulatory oversight, contribute significantly to vegetation loss**,** soil compaction, and increased surface runoff (Sahnoune et al., 2018).

Overgrazing is one of the most critical anthropogenic pressures in the region. It leads to persistent depletion of vegetative cover and the formation of bare, crusted soils, especially during extended droughts when plant regeneration is limited. The cumulative effects of animal trampling, biomass removal, and root exposure reduce the soil's resistance to raindrop impact and flow concentration, intensifying erosion processes (Amraoui et al., 2016).

Urban expansion, particularly near the town of Boughezoul, along with the development of transport infrastructure, has altered natural drainage patterns and destabilized slopes. Activities such as road construction, land grading, and drainage diversion frequently result in localized accelerated erosion, including gully formation and down stream sediment deposition(Cherifi et al., 2020). Additionally, unsustainable agricultural practices including deep till age on slopes, monoculture without crop rotation, and the absence of erosion control measures contribute to the deterioration of soil structure, reduction in organic matter, and enhanced runoff generation. For erosion modeling and conservation planning, it is essential to **s**ystematically map and quantify the spatial distribution and intensity of land-use pressures. Recent remote sensing-base assessments (Guettouche et al., 2022) underscore the utility of high-resolutionl and use classification and change detection techniques for identifying areas of anthropogenic erosion risk. Integrating socio-environmental dynamics into erosion models provides a more holistic understanding of land degradation. It also forms the basis for context-specific, sustainable land management policies particularly critical in environmentally vulnerable landscapes like the Boughezoul watershed.

2.4 Watershed Morphometry and Hydrological Behavior

2.4.1 Geometric Characteristics

The watershed spans 2,817.97 km² with a perimeter of 340.47 km. Its Gravelius Index (KG), calculated as follows:

$$K_G = \frac{P}{2\sqrt{\pi A}} \approx 1.8 \quad \ldots\ldots\ldots\ldots\ldots\ldots\ldots\ldots\ldots\ldots \text{(2)}$$

This value suggests an elongated basin shape, typically associated with delayed peak discharge and prolonged runoff. The watershed's geometry can be approximated by a rectangle measuring 152.10 km by 18.53 km, which simplifies hydrological modeling.

2.4.2 Drainage Network Characteristics

The Boughezoul watershed exhibits a drainage pattern ranging from dendritic to trellis, primarily influenced by lithological variations and slope gradients (Montgomery & Dietrich,

1992). According to Strahler's classification, it features a well-developed, multi-order stream network (Strahler, 1957). The drainage density, defined as the total stream length per unit area, is relatively high, indicating a landscape prone to rapid runoff, especially in areas with sparse vegetation cover, which further accelerates overland flow and sediment transport (Horton, 1945).

The Boughezoul reservoir has experienced significant sedimentation, with the average annual sedimentation rate estimated at approximately 0.67 million m^3. This has led to a reduction in storage capacity, from 55 million m^3 in 1934 to approximately 15 million m^3 by 2011 (Remini et al., 2015). The sediment load primarily results from upstream erosion, exacerbated by the dense drainage network and inadequate land management practices. Although not a direct hydrological variable, the hypsometric curve suggests that the basin is in a mature geomorphic stage, where erosion and deposition processes are generally balanced, particularly in the midstream and downstream reaches (Pike & Wilson, 1971; Chorley et al., 1985).

These morphometric and sedimentological characteristics are crucial for calibrating hydrological and erosion models, such as the Revised Universal Soil Loss Equation (RUSLE). Recent advances in remote sensing and GIS have improved the integration of these parameters into spatial modeling. Furthermore, combining RUSLE with machine learning techniques, such as Long Short-Term Memory (LSTM) networks and Random Forest, has proven effective in regional-scale erosion risk assessments (Ahmad et al., 2023). These approaches assist in identifying priority sub-watersheds for targeted conservation interventions.The stream network map (Figure 2.6) illustrates the spatial structure of the drainage system, derived from DEM-based flow accumulation modeling. The dendritic and trellis patterns reflect underlying lithological controls and slope configurations. Main channels are concentrated along the central and northern sectors, corresponding to zones with steeper gradients and higher drainage density. These channels form sediment transport corridors that align with observed erosion hotspots, confirming the hydrological sensitivity of these areas.

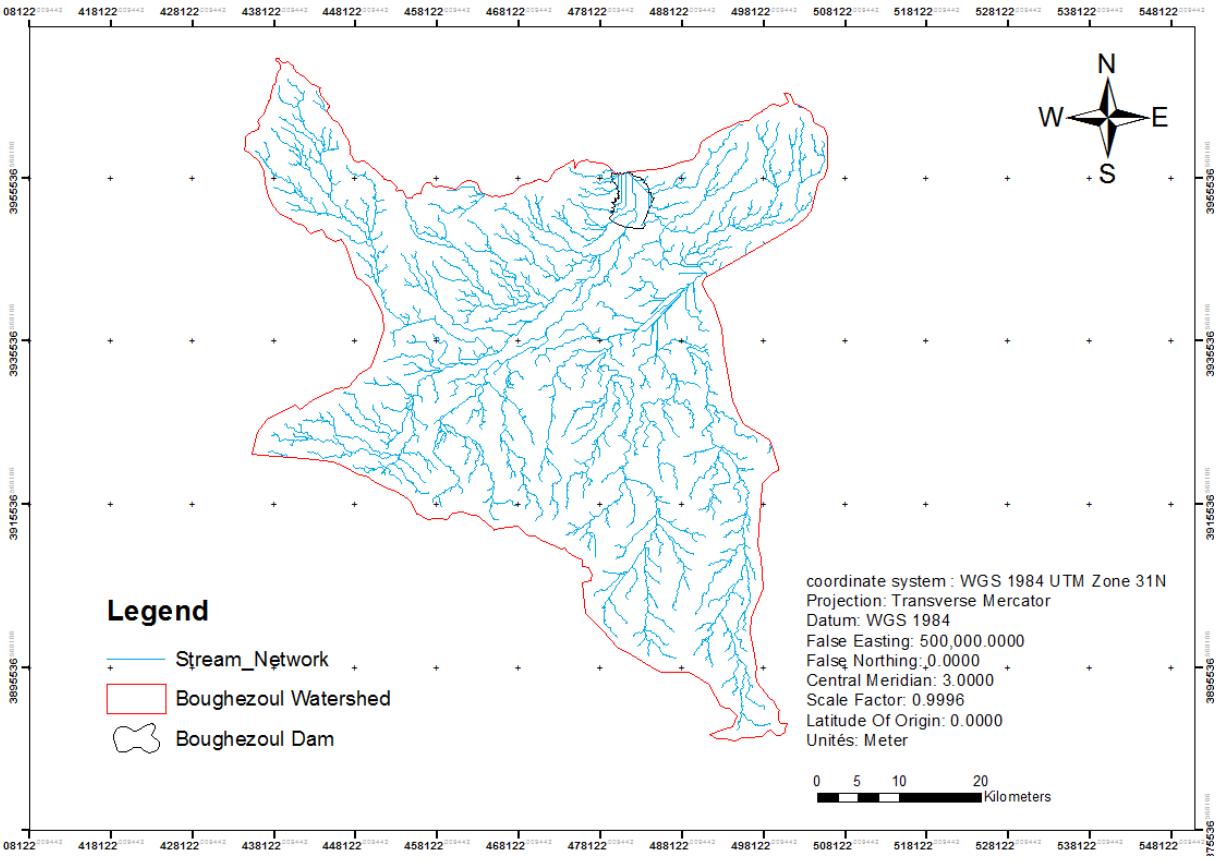

Figure 2.6: Stream Network Map of the Boughezoul Watershed.

The table below summarizes the key morphometric parameters that define the physical and hydrological characteristics of the Boughezoul watershed.

Table 2.1: Geographical and Morphometric Parameters of the Boughezoul Watershed.

Parameter	**Unit**	**Value**	**Interpretation**
Area (A)	km²	2,817.97	Watershed size
Perimeter (P)	km	340.47	Basin boundary length
Gravelius Index (KG)	–	1.80	Elongated basin; delayed, sustained runoff
Equivalent Rectangle	km	152.10 × 18.53	Simplified geometry for modeling
Elevation Range	m	619 – 1,712	Topographic variability
Average Elevation	m	~1,200	Median altitude
Average Slope	%	79.12	High slope promotes runoff and erosion
Drainage Pattern	–	Dendritic/Trellis	Controlled by lithology and slope
Drainage Density	–	High	High potential for rapid runoff
Hypsometric Curve	–	Mature	Balanced erosion deposition dynamics

2.5 Conclusion

The Boughezoul watershed presents a complex and heterogeneous landscape shaped by its semi-arid climate, varied topography, and lithological diversity. Its geographic position between the Tellian Atlas and Saharan zones, along with its geomorphological maturity, contributes to diverse erosion processes and sediment dynamics. The interplay of steep slopes, weakly consolidated soils, and irregular rainfall patterns enhances the region's vulnerability to runoff and soil degradation.

The watershed's physical and hydrological features such as drainage density, hypsometric structure, and soil types highlight the importance of spatially detailed analysis for erosion modeling. Human activities, particularly overgrazing, unsustainable farming, and urban expansion, further aggravate land degradation and sediment transport. Understanding these natural and anthropogenic factors is essential for developing targeted, context-specific erosion control strategies.

Chapter 3
Materials and Methods

3 Chapter 3 Materials and Methods

3.1 Materials and data used

This study relied on a range of datasets and software tools to support the spatial modeling and analysis of soil erosion in the Boughezoul watershed. The primary materials and data sources are described below.

3.1.1 Digital Elevation Model (DEM)

The Digital Elevation Model (DEM) used in this study was derived from the ASTER Global DEM, with a native spatial resolution of approximately 38.2 meters. The dataset was downloaded via Global Mapper software and used to extract key hydrological and morphological parameters essential for terrain analysis. The following preprocessing steps were conducted in ArcGIS 10.4:

- Filling sinks to correct surface depressions;
- Generating slope and flow direction rasters;
- Computing flow accumulation to derive the LS factor (slope length and steepness), a critical input for the RUSLE model.

3.1.2 Rainfall and Climate Data

Rainfall data were obtained using the Climatic Research Unit Time Series (CRU TS) dataset, a globally recognized gridded climate dataset providing monthly precipitation records at 0.5° spatial resolution. This dataset was accessed through the Google Earth interface, where observation points across and around the Boughezoul watershed were manually identified and geolocated to ensure local representativeness. Monthly precipitation values were extracted for the 2014–2024 period, generating a spatially distributed rainfall dataset suitable for estimating the rainfall erosivity factor (R) in the RUSLE model.

The use of CRU TS data ensured consistency, reliability, and temporal coverage, especially in a context where in-situ pluviometric data were scarce or incomplete. This method provided a practical and scientifically robust basis for modeling rainfall erosivity in a semi-arid environment like the Boughezoul watershed.

3.1.3 Soil and Land Cover Data

Soil data were extracted from the Digital Soil Map of the World (DSMW), published by the FAO in shapefile format. The attribute table included sand, silt, clay, and organic carbon

content. These parameters were used to calculate the K factor (soil erodibility) for each soil unit.Land cover information was derived from the ESA WorldCover 2020 dataset, offering global coverage at 10-meter resolution. The data were reclassified in ArcGIS 10.4 to assign C factor values, based on established literature. This reclassification reflects the protective role of vegetation and surface cover in limiting soil erosion.

3.1.4 Software Tools

The following software tools were used throughout the data processing and analysis stages:

- ArcGIS 10.4 for spatial analysis, raster processing, and map algebra operations;
- Global Mapper for DEM acquisition and terrain data preparation;
- Microsoft Excel for empirical calculations of the R factor;
- Google Earth for geolocation and referencing of rainfall observation points.

All spatial datasets were projected to WGS84 / UTM Zone 31N and resampled to a common resolution of 30 meters to ensure consistency across inputs. The Boughezoul watershed boundary was used to clip all layers, and thematic data were rasterized or smoothed as needed. The processed factor maps were subsequently assembled and overlaid using map algebra tools in ArcGIS 10.4 to generate the final RUSLE-based soil erosion risk map.

3.2 OVERVIEW OF METHODOLOGICAL APPROACH

This study applies the Revised Universal Soil Loss Equation (RUSLE) within a Geographic Information System (GIS) to quantify soil erosion risk in the Boughezoul watershed. RUSLE estimates average annual soil loss based on five factors: rainfall erosivity (R), soil erodibility (K), topography (LS), cover-management (C), and support practices (P). Each factor was derived from spatial datasets using geostatistical and raster-based analysis in ArcGIS 10.4.

To improve the spatial accuracy of erosion risk assessment, several topographic and hydromorphometric indices were calculated from the Digital Elevation Model (DEM). These include the Compound Topographic Index (CTI), Stream Power Index (SPI), Stream Density Index (SDI), and Terrain Ruggedness Index (TRI). These indices help capture variations in slope, flow accumulation, and terrain complexity, offering additional insight into areas with high erosion potential.In addition to soil loss estimation, a Sediment Delivery Ratio (SDR) model was used to estimate the proportion of eroded soil likely to reach the main drainage network. SDR was calculated using a slope-based empirical approach. This allowed the conversion of soil loss values into sediment yield (SY), providing a more realistic estimation of sediment transport.

The methodological workflow followed five main steps:

1. Collection and preparation of topographic, climatic, and soil data;
2. Spatial preprocessing and standardization of input layers in GIS;
3. Calculation of RUSLE factors and terrain indices (LS, TRI, SPI, etc.);
4. Application of the SDR model and estimation of sediment yield;
5. Integration of all outputs to produce a final erosion risk map.

The RUSLE model and auxiliary terrain analysis were implemented in a raster-based GIS environment using spatially localized inputs and empirical formulations adapted to the specific conditions of the Boughezoul watershed. All factors were computed independently in ArcGIS 10.4 and integrated using map algebra and spatial modeling tools to produce the final erosion risk and sediment yield outputs.

Figure 3.1 summarizes the full methodological process, from data preparation to erosion and sediment yield mapping.

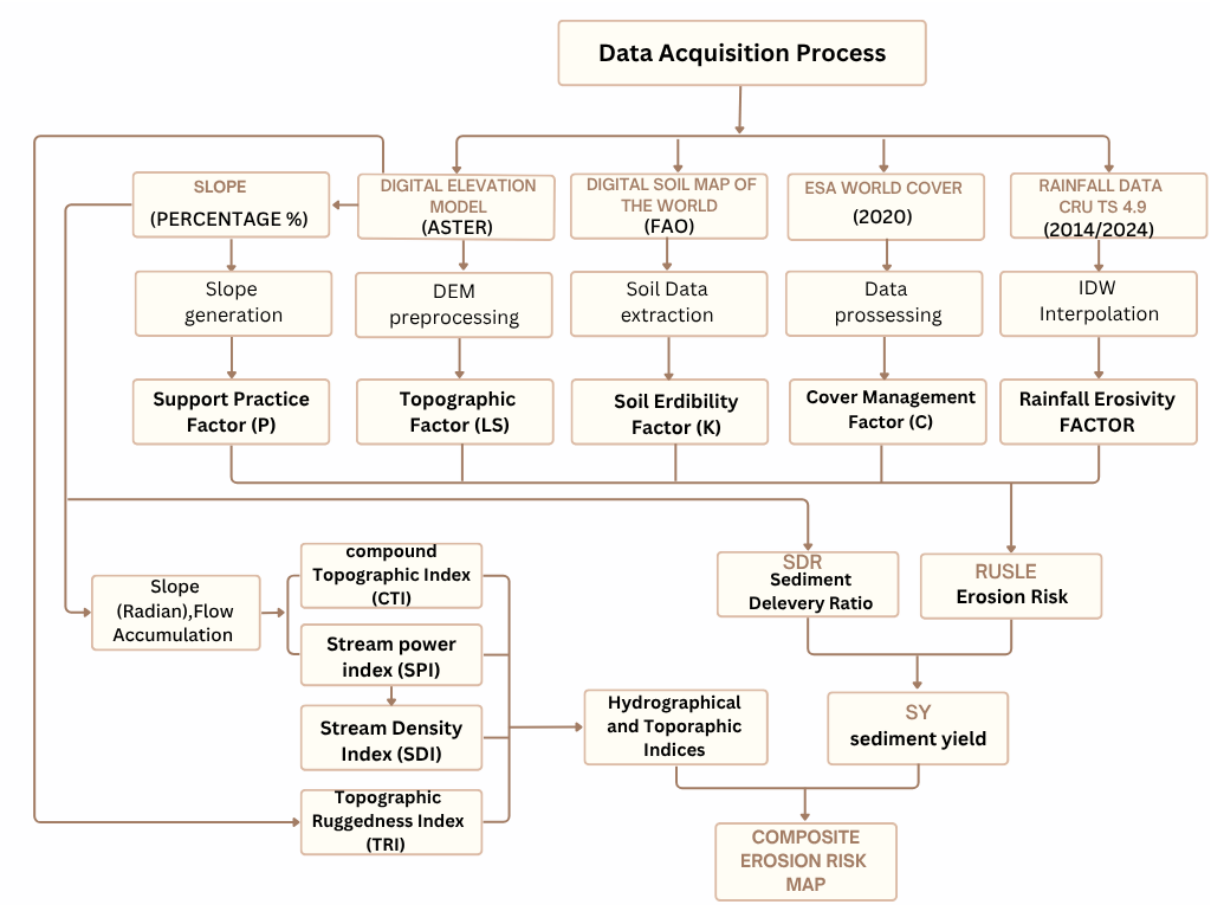

Figure 3.1: Methodological workflow for soil erosion and sediment yield modeling using RUSLE and GIS-based terrain analysis in the Boughezoul watershed.

3.2.1 Estimation of RUSLE Model Parameters

3.2.1.1 R factor(Rainfall Erosivity)

The R factor represents the erosive potential of rainfall and is typically derived from high-resolution precipitation intensity data. However, in semi-arid regions such as the Boughezoul watershed, detailed pluviograph records are often unavailable. Consequently, simplified empirical equations based on Mean Annual Rainfall (MAR) of 8 rainfall stationare commonly employed as an alternative (Renard et al., 1997).Due to the low density of meteorological stations and the absence of high-frequency rainfall data, the following empirical equation was adopted:

$$R = 0.5 \times MAR \quad \text{..... (3)}$$

This approach is supported by recent Algerian studies focusing on watersheds with annual precipitation ranging from 300 to 500 mm and moderate relief characteristics (Bencheikh-Lehocine et al., 2020). Monthly rainfall data were manually collected for the 2014–2024 period using Google Earth, referencing 10 spatially distributed observation points in and around the Boughezoul watershed. The MAR values were then computed and spatially interpolated using the Inverse Distance Weighting (IDW) method in ArcGIS 10.4 to generate a continuous raster layer representing rainfall erosivity (R factor). Although this empirical method does not account for rainfall intensity or intra-annual variability, it remains widely used in semi-arid environments where detailed pluviometric data are scarce. In the case of the Boughezoul watershed, the lack of pluviograph stations and the limited spatial coverage of conventional meteorological networks make this approach one of the most practical and context-appropriate alternatives. Under these conditions, the method provides a reliable approximation of rainfall erosivity for regional-scale erosion modeling. The workflow implemented in ArcGIS ModelBuilder for the calculation of the R factor is presented in Figure 3.2.

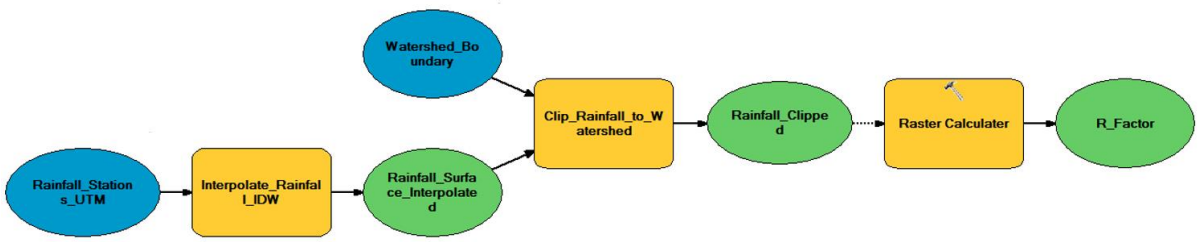

Figure 3.2: Workflow implemented in ArcGIS ModelBuilder for calculating the rainfall erosivity factor (R).

Based on the interpolated MAR values and the applied empirical equation, the resulting rainfall erosivity map is shown in Figure 3.3, highlighting the spatial variability of erosive potential within the watershed.

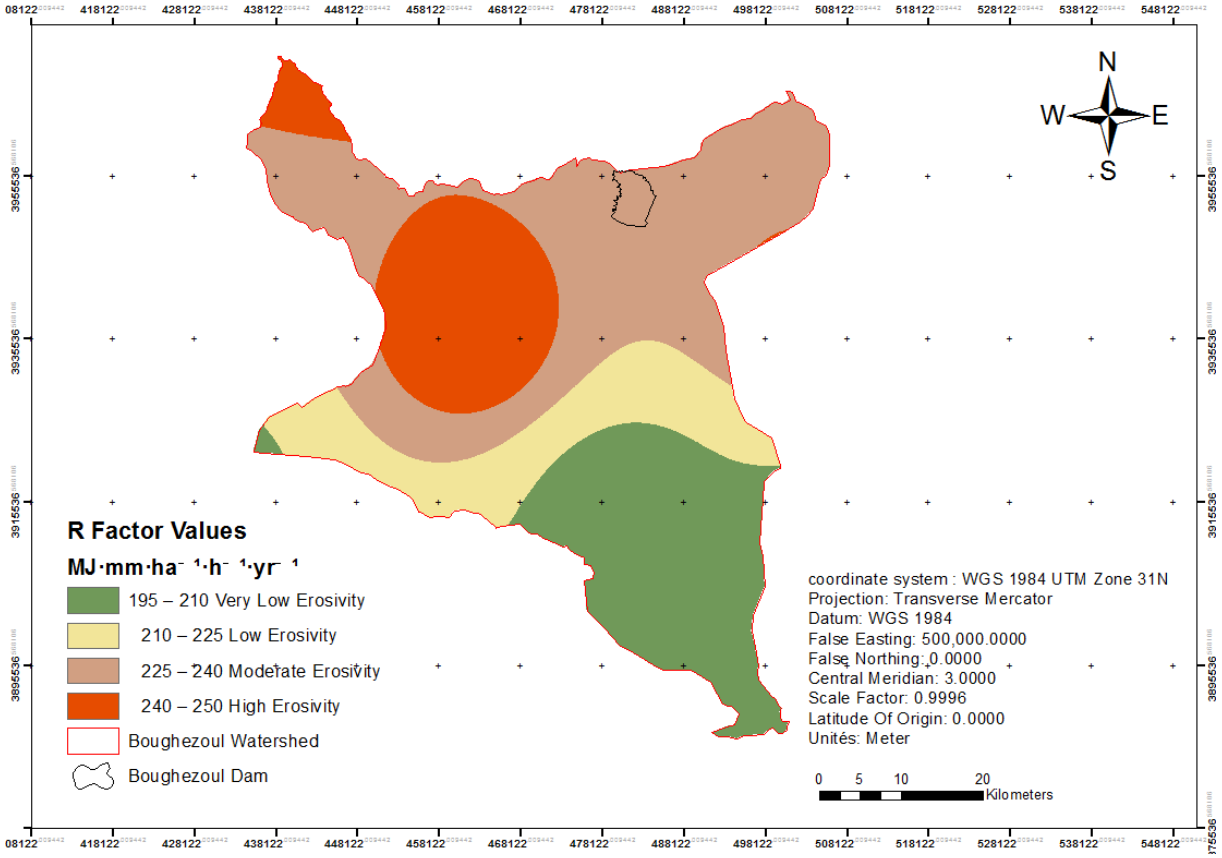

Figure 3.3: Rainfall Erosivity Factor Map for the Boughezoul Watershed.

The R factor map shows rainfall erosivity values (MJ·mm/ha·h·yr) across the Boughezoul watershed, highlighting the spatial variability of precipitation's erosive potential. Using the Jenks natural breaks classification method, the map delineates four distinct erosivity zones:

Very Low Erosivity (195 – 210 MJ·mm/ha·h·yr): Located primarily in the southern and southeastern areas, these zones experience reduced rainfall intensity and gentle slopes, resulting in minimal erosive force.

Low Erosivity (210 – 225 MJ·mm/ha·h·yr): Found mostly in central plateau and mid-elevation zones, these areas receive moderate rainfall, often mitigated by vegetation cover and low gradients, thus limiting erosion.

Moderate Erosivity (225 – 240 MJ·mm/ha·h·yr): Observed in the mid-northern and western parts of the watershed, where increased rainfall intensity and patchy vegetation contribute to greater erosive potential.

High Erosivity (240 – 250 MJ·mm/ha·h·yr): Concentrated in the north-central region, this zone is characterized by high-intensity rainfall combined with steeper slopes, leading to elevated erosion risks and identifying a priority area for conservation interventions.

This map plays a crucial role in the RUSLE modeling framework, offering a detailed spatial perspective on the natural erosive forces across the watershed. When combined with other RUSLE factors, it significantly enhances the accuracy of erosion risk assessments and land management planning.

3.2.1.2 K Factor (Soil Erodibility)

The K factor expresses the inherent susceptibility of soil particles to detachment and transport by rainfall and surface runoff. It is primarily influenced by soil texture (sand, silt, and clay proportions) and organic matter content. In the context of the RUSLE model, the K factor is typically estimated using the Wischmeier nomograph or related empirical equations. It was selected due to its compatibility with the available data and its proven reliability in erosion modeling. This formula accounts for the physical properties of soils in the Boughezoul watershed, particularly texture and organic carbon content.

The following simplified version of the Wischmeier equation was applied:

$$K = 0.1317 \times \frac{(SILT \times (100 - CLAY))^{0.2}}{(SAND + SILT)^{0.3}} \times \left(1 - 0.25 \times \frac{OC}{100}\right) \quad \text{(4)}$$

Where:

- K is the soil erodibility factor (in t·ha·h/ha·MJ·mm),
- silt and clay and sand are expressed as percentages (%),
- OC is the organic carbon content (%).

Soil data were extracted from the Digital Soil Map of the World (DSMW). These values were joined in ArcGIS 10.4 to the soil polygon layer. A rasterization process at 30-meter resolution was then conducted to generate a spatially continuous K factor map. The resulting raster reflects the variability of soil erodibility across the watershed, driven by differences in texture and organic matter content.

The resulting K factor values for the main soil types present in the watershed are shown in the following Table.

Table 3.1: Soil erodibility (K factor) values for major soil types in the Boughezoul watershed.

Soil Type	K Factor
Calcic Cambisols	0.2038
Lithosols	0.5289
Calcic Yermosols	0.1469
Orthic Solonchaks	0.2322
Calcic Xerosols	0.3979

These values are consistent with typical erodibility ranges observed in Mediterranean semi-arid soils, where lithosols and xerosols tend to exhibit higher susceptibility to erosion due to their shallow depth and weak structure. The observed variation in K values highlights the influence of soil propertiesparticularly texture and organic matteron erodibility within the Boughezoul watershed.The geoprocessing steps used to calculate and rasterize the K factor in ArcGIS are summarized in the ModelBuilder workflow shown in Figure 3.4.

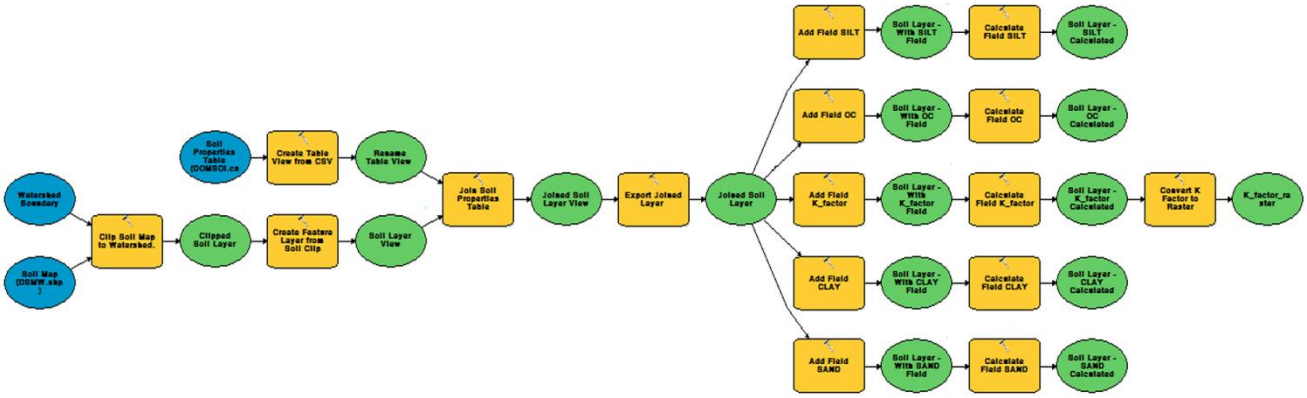

Figure 3.4: ArcGIS ModelBuilder workflow for calculating the soil erodibility factor (K).

The resulting spatial distribution of soil erodibility across the Boughezoul watershed is illustrated in Figure 3.5.

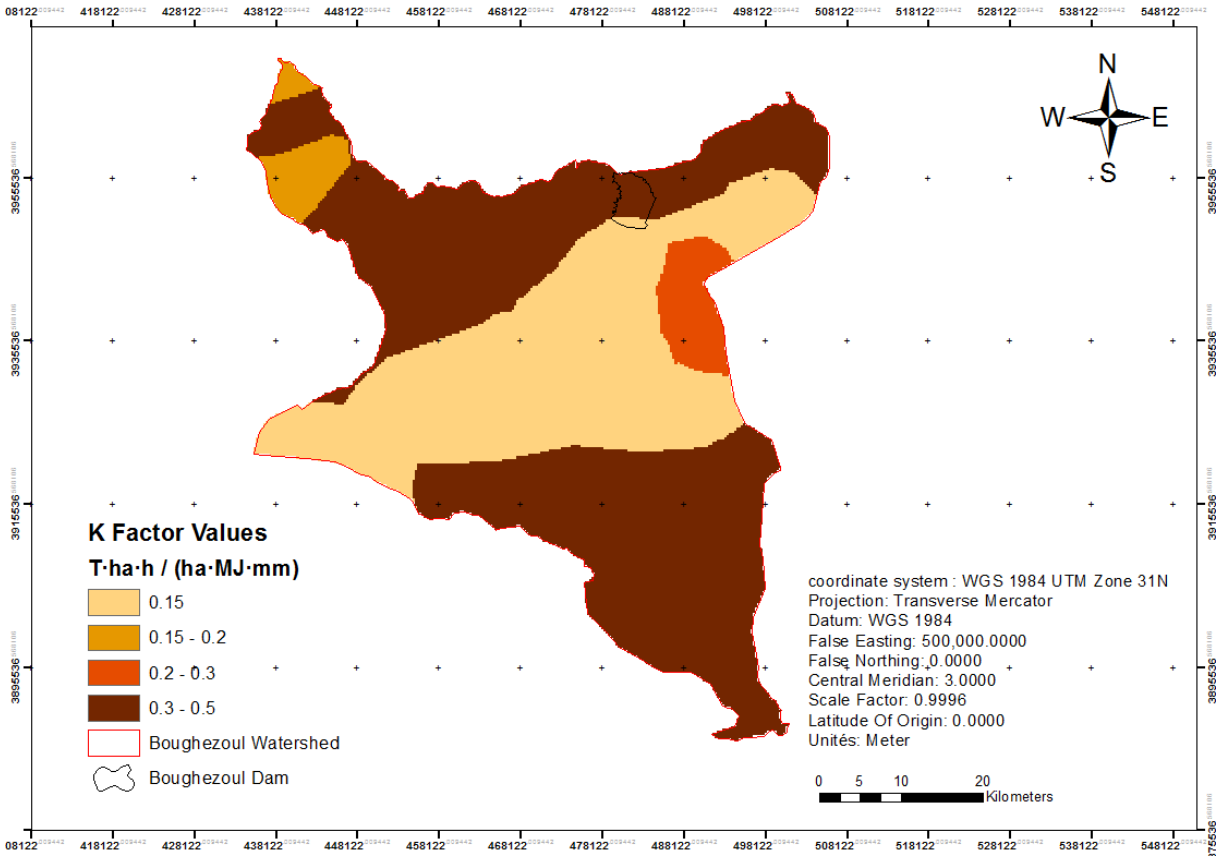

Figure 3.5: Soil erodibility factor (K) map for the Boughezoul watershed.

The K factor map represents the soil's inherent susceptibility to erosion under standard conditions of rainfall and runoff, independent of vegetation cover and slope gradient. It reveals spatial patterns driven primarily by soil texture, structure, and organic matter content. Four erodibility classes were identified based on the classified raster layer:

Very Low Erodibility (0.15 t·ha·h/ha·MJ·mm): Concentrated in the northern and southwestern regions, these soils are characterized by high clay content or strong aggregation, which provide greater resistance to detachment. These zones are typically associated with Calcic Yermosols or compacted soil units.

Low Erodibility (0.15 – 0.2 t·ha·h/ha·MJ·mm): Dominant in the central watershed, these soils exhibit moderate cohesion and organic matter levels, offering partial protection against erosion. They are commonly found in Lithosols and Cambisols.

Moderate Erodibility (0.3 – 0.3 t·ha·h/ha·MJ·mm): Observed in southeastern slopes and shallow depressions, these areas show higher silt content and reduced organic matter, increasing their vulnerability under elevated erosivity (R) or topographic (LS) values.

High Erodibility (0.3 – 0.5 t·ha·h/ha·MJ·mm): Located in the southeastern and northeastern zones, these soils are typically sandy or silty with weak structural cohesion, making them highly susceptible to erosion even under moderate rainfall conditions.

The K factor map reflects the geomorphological and pedological variability within the Boughezoul watershed and plays a critical role in the RUSLE model by modulating the combined effects of rainfall erosivity and slope-related factors.

3.2.1.3 LS Factor (Slope Length and Steepness)

The LS factor quantifies the influence of slope length and steepness on soil erosion processes. It reflects how water accumulates and accelerates on sloped surfaces, increasing the detachment and transport capacity of runoff. For this study, the Moore and Burch (1986) equation was selected due to its compatibility with raster-based GIS analysis and its robustness across heterogeneous terrain. Given the topographic variability of the Boughezoul watershed and the availability of an ASTER DEM with a spatial resolution of 38.2 meters, the Moore & Burch method was deemed appropriate as it offers a balance between computational efficiency and spatial accuracy.

The LS factor was calculated using the following equation:

$$\mathbf{LS} = [(\boldsymbol{FlowAccum} \times \boldsymbol{CellSize})/\mathbf{22.13}]^{\mathbf{0.4}} \times \frac{[\boldsymbol{sin}(\boldsymbol{Slope}\ (°) \times \frac{\boldsymbol{\pi}}{\mathbf{180}}]}{\mathbf{0.0896^{1.3}}} \quad \textbf{(5)}$$

Where:

- Flow Accumulation is the upslope contributing area (in number of cells),
- Cell Size is the spatial resolution of the raster (38.2 m),
- Slope is the slope angle in degrees, derived from the DEM.

Slope and flow accumulation rasters were generated from the ASTER DEM using ArcGIS 10.4 spatial analyst tools. The equation was implemented using map algebra in raster calculator to produce a continuous LS factor map at 30-meter resolution.

The LS factor calculation process was automated in ArcGIS ModelBuilder, as shown in Figure 3.6.

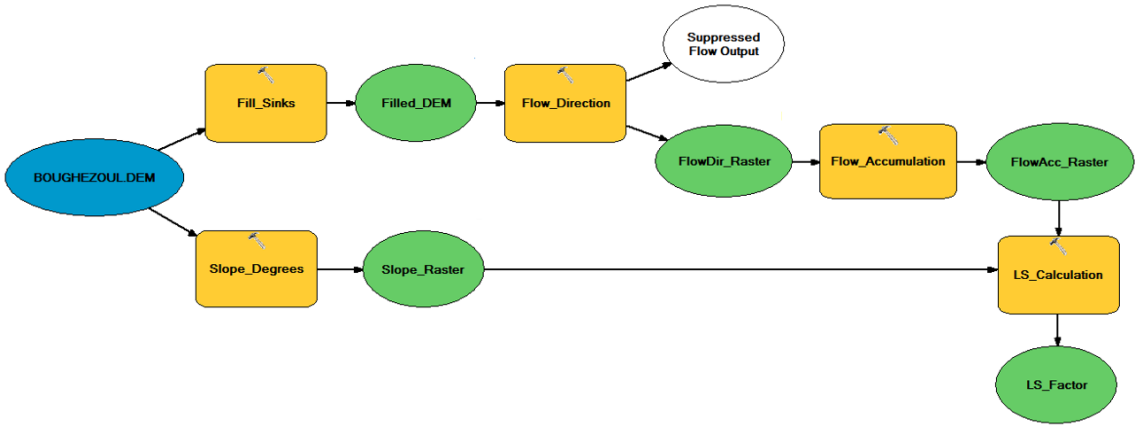

Figure 3.6: ArcGIS ModelBuilder workflow for calculating the LS factor.

The resulting spatial distribution of the LS factor is presented in Figure 3.7.

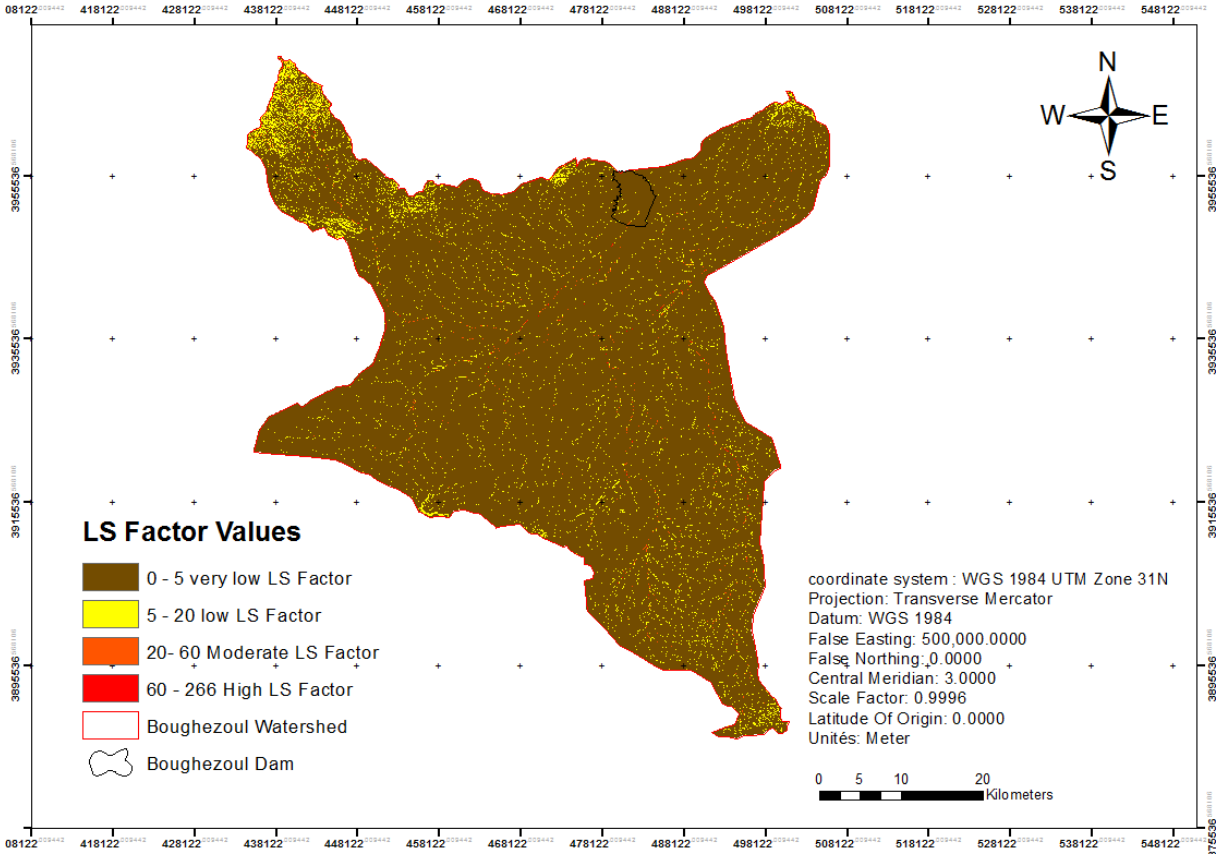

Figure 3.7: Topographic factor (LS) map for the Boughezoul watershed.

The LS factor map (dimensionless) illustrates the combined influence of slope length and slope gradient on soil erosion potential. It captures the gravitational effect on erosion

processes such as sheet and rill erosion, thereby emphasizing topographic control over surface runoff dynamics. Four classes of LS values were identified across the watershed:

Very Low LS (0 – 5): Located in flat valleys, depressions, and near-stream zones, these areas exhibit minimal slope and flow velocity. Erosion potential is negligible, although such zones may act as sediment deposition areas for upstream transport.

Low LS (5 – 20): Found in gently sloping plains and mildly inclined fields, these areas experience slow overland flow, with limited capacity to detach soil unless compounded by intense rainfall or poor vegetation cover. Erosional risk in these areas is primarily related to splash erosion and surface sealing.

Moderate LS (20 – 60): Typically observed in transitional zones between upper slopes and mid-elevation regions. The combination of increasing slope and flow length enhances flow energy, promoting sheet erosion and potential rill formation. These areas often coincide with terrain concavities where water converges naturally.

High LS (60 – 266): Concentrated on steep escarpments, hillslopes, and narrow valleys. These areas feature extended flow paths and steep gradients, generating high-velocity runoff. As a result, they are prone to severe erosion processes such as gullying and slope instability, particularly in the absence of adequate land management.

The LS factor map provides key insights into the topographic drivers of erosion within the Boughezoul watershed. It plays a critical role in the RUSLE framework by identifying terrain-induced erosion risks, independent of rainfall erosivity or soil type.

3.2.1.4 C *Factor (Cover Management)*

The C factor reflects the effect of vegetation cover and land use on soil erosion processes. It accounts for how surface conditions such as canopy cover, plant density, and agricultural activity either protect the soil or expose it to erosive forces. Remote sensing offers an efficient and standardized means of estimating the C factor based on land cover classification.

For this study, the ESA WorldCover 2020 dataset (10 m spatial resolution) was used to derive land cover information. This dataset offers high-resolution, globally consistent land use data. C factor values were assigned to land cover classes based on established values in the literature (Wischmeier& Smith, 1978; Panagos et al., 2015). The reclassification used is presented in Table 3.2.

Table 3.2: Assigned C values based on ESA WorldCover 2020 land cover types.

Land Cover Type	ESA Code	C Value
Tree Cover	**10**	**0.001**
Shrubland	**20**	**0.003**
Grassland	**30**	**0.05**
Cropland	**40**	**0.2**
Evergreen Tree Cover	**50**	**0.001**
Bare/SparseVegetation	**60**	**0.001**
Wetlands	**80**	**0.0**

The raster land cover map was resampled to 30-meter resolution and clipped to the watershed boundary. The resulting raster was reclassified using ArcGIS 10.4 to assign C values to each land cover type, producing a spatially explicit cover-management factor layer.

The classification and reprocessing steps for generating the C factor map were implemented in ArcGIS ModelBuilder, as illustrated in Figure 3.8.

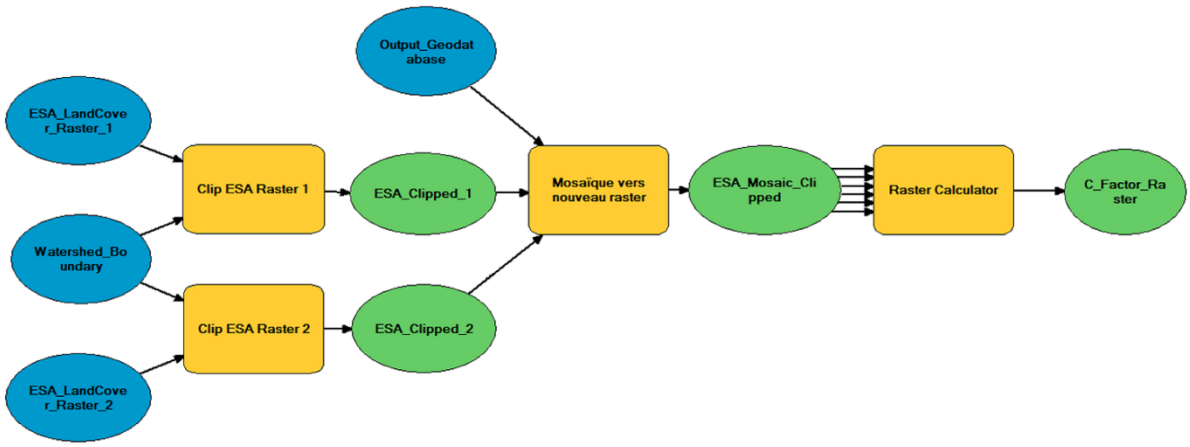

Figure 3.8: ArcGIS ModelBuilder workflow for calculating the cover-management factor (C).

The spatial distribution of the C factor across the Boughezoul watershed is presented in Figure 3.9.

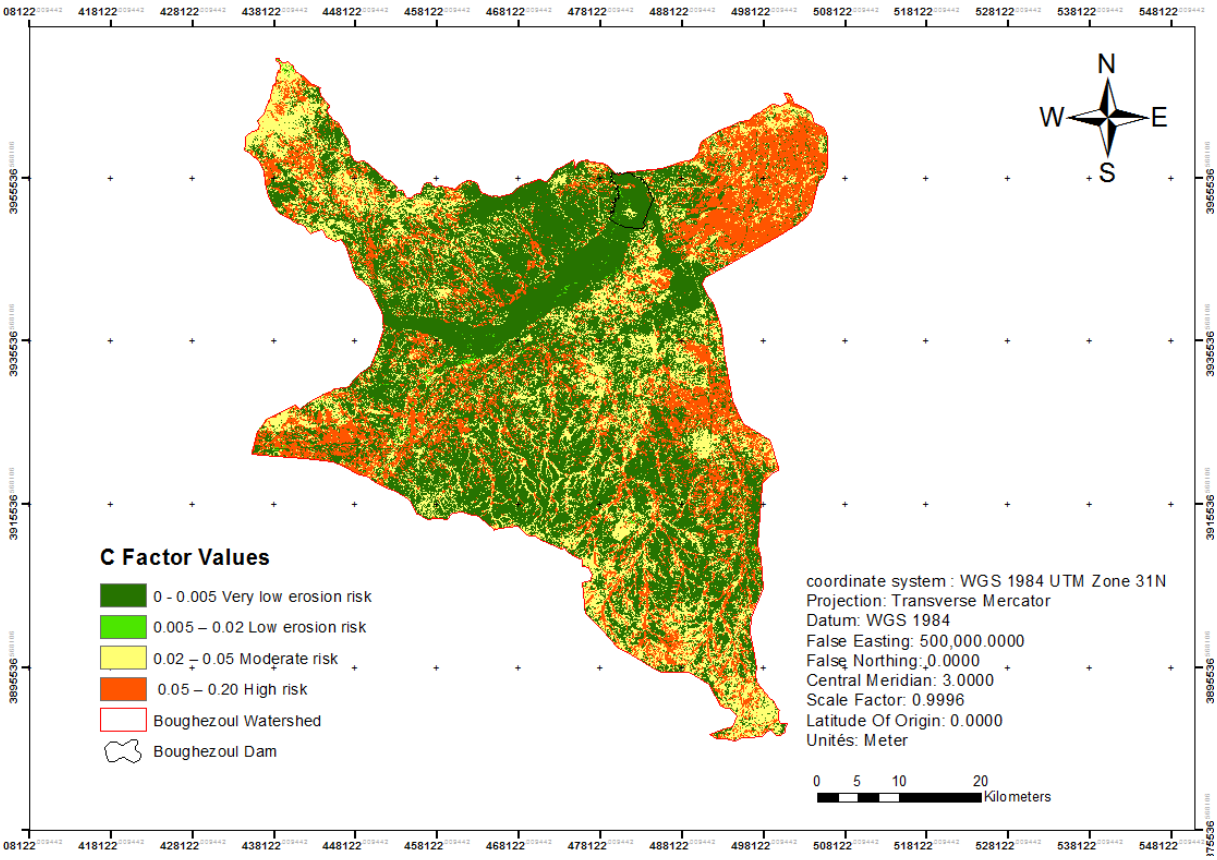

Figure 3.9: Cover-management factor (C) map for the Boughezoul watershed.

The C factor map (values ranging from 0 to 1) quantifies the protective effect of vegetation cover, land use, and crop management practices against soil erosion. Lower C values indicate strong protective capacity, while higher values reflect greater vulnerability to erosive forces. Based on reclassified ESA WorldCover data, the following land cover-based C classes were identified:

Very Low C (0 – 0.005): Located in densely forested areas, perennial vegetation zones, or well-managed permanent crops. These areas provide excellent soil protection, effectively minimizing erosioneven under high rainfall or steep slope conditions.

Low C (0.005 – 0.02): Representing shrubland, grassland, or semi-natural covers, these areas offer partial protection. Erosional processes may occur during extended dry periods, overgrazing, or reduced vegetation density.

Moderate C (0.02 – 0.05): Commonly found in cropland, especially during off-season or between planting cycles. With limited vegetative cover, these areas are vulnerable to rainfall impact, leading to surface sealing, crusting, and early-stage rill erosion.

High C (0.05 – 0.20): Associated with bare soils, recently cleared land, fallow fields, or construction zones. These surfaces are highly susceptible to splash, sheet, and rill erosion and often require targeted soil conservation or re-vegetation measures.

The C factor plays a key role in modulating the impact of climatic (R) and topographic (LS) forces within the RUSLE framework. Areas with elevated SPI or slope values may experience significantly increased soil loss where C values are moderate to high.

3.2.1.5 P Factor (Support practice)

The P factor reflects the effect of soil conservation practices that reduce the velocity of surface runoff and minimize soil erosion. These include techniques such as contour plowing, strip cropping, and terracing. In the absence of detailed, spatially explicit field data on conservation practices, slope-based estimation offers a validated alternative approach, particularly in semi-arid and Mediterranean environments.

In this study, no conservation infrastructure or land management map was available for the Boughezoul watershed. As such, P values were assigned based on slope gradients, following recommendations from the USDA Soil Conservation Service and RUSLE guidelines adapted for Mediterranean contexts. Slope percentage was derived from the ASTER DEM and reclassified using Jenks natural breaks. Corresponding P values were then assigned to each slope class as summarized in Table3.4.

Table 3.4: Assigned P values based on slope classes for the Boughezoul watershed.

Slope Range (%)	**P Value**	**Interpretation**
0 – 1.73	**0.6**	**Low slope – basic management assumed**
1.73 – 3.62	**0.5**	**Gentleslope – likelysupported**
3.62 – 7.09	**0.5**	**Moderateslope**
7.09 – 13.23	**0.7**	**High slope – minimal practices**
13.23 – 40.17	**1.0**	**Steep slope – no support assumed**

The slope raster was reclassified in ArcGIS 10.4 using these P values to produce a spatially distributed support practice layer for RUSLE. The reclassification procedure and spatial processing were implemented in ArcGIS ModelBuilder, as illustrated in Figure 3.10.

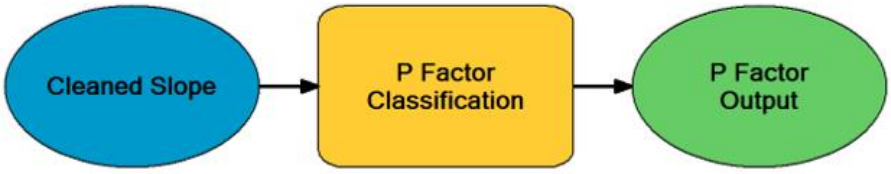

Figure 3.10: ArcGIS ModelBuilder workflow for calculating the support practice factor (P).

The spatial distribution of the P factor across the Boughezoul watershed is shown in Figure 3.11.

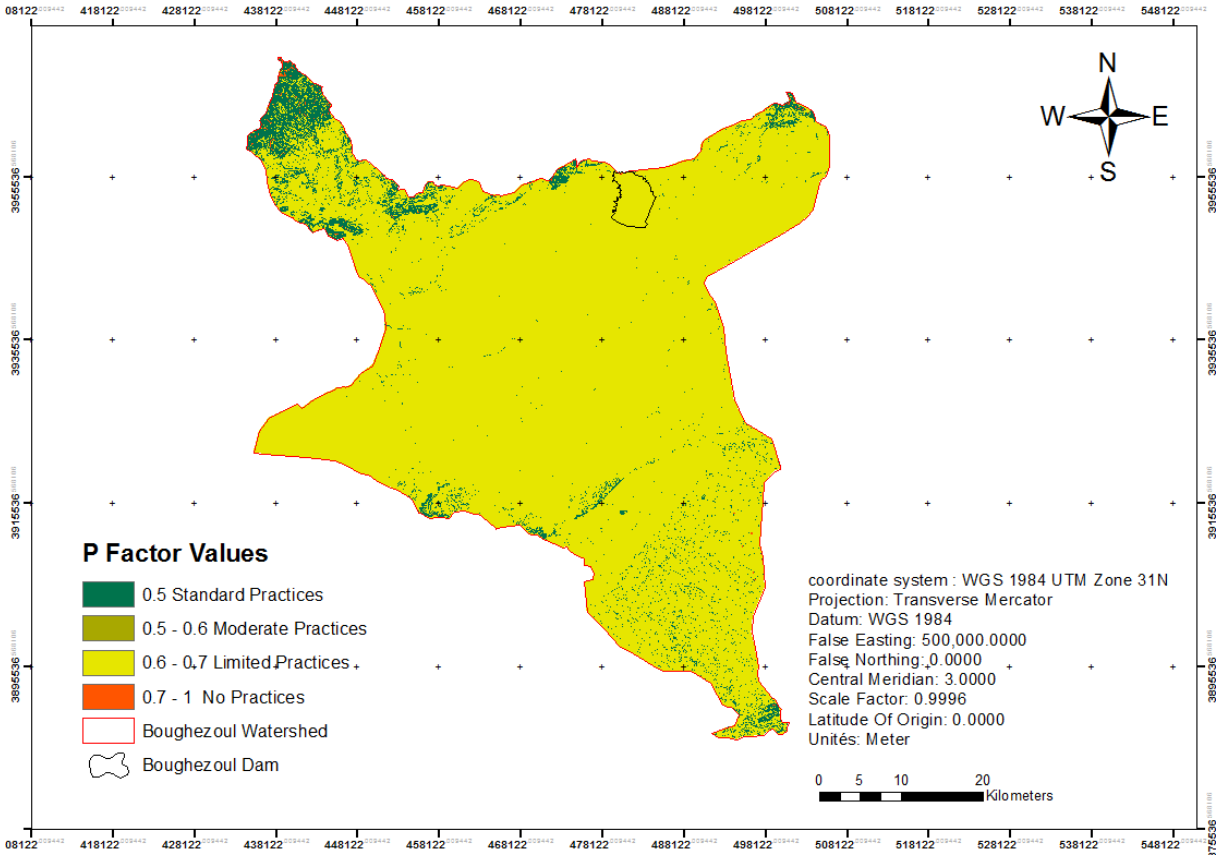

Figure 3.11: Support practice factor (P) map for the Boughezoul watershed.

The P factor map (values ranging from 0 to 1) illustrates the spatial distribution of erosion control effectiveness resulting from support practices such as contour farming, strip cropping, or terracing. Lower values indicate better protection against soil loss, while higher values reflect the absence or inefficiency of conservation measures. Four protection classes were identified:

Standard Practices (0.5): Found in flat to gently sloping areas where effective conservation practices are assumed, such as contour plowing, vegetative buffers, or basic terracing. These practices substantially reduce runoff and erosion risk.

Moderate Practices (0.5 – 0.6): Observed in areas with modest slopes where partial water flow control is expected (e.g., vegetative strips or basic contouring). These areas show moderate erosion control, though their effectiveness may diminish under intense rainfall events.

Limited Practices (0.6 – 0.7): Found in zones where conservation measures are minimal or informal. Erosion is passively reduced through temporary vegetation cover or crop residues, but structured support practices are lacking.

No Practices (0.7 – 1.0): Concentrated in steep terrains and degraded lands with no implemented conservation strategies. These areas are highly vulnerable to erosion, especially when combined with high LS or C values, and should be prioritized for targeted intervention.

The P factor is critical in the RUSLE framework, as it identifies where human intervention can effectively mitigate erosion and improve overall soil stability, particularly in synergy with topographic and climatic factors.

3.3 Sediment Yield Estimation Using SDR

While the RUSLE model provides estimates of gross soil loss (*A*) at the hillslope scale, it does not account for sediment retention and deposition occurring during sediment transport across the landscape. To overcome this limitation, the Sediment Delivery Ratio (SDR) is introduced as a correction factor that quantifies the proportion of eroded material that actually reaches the watershed outlet (Vanoni, 1975). The sediment yield (*SY*) is then calculated using the following relationship:

$$SY = A \times SDR \quad \text{..... (6)}$$

This formulation enables the conversion of localized erosion values into spatially distributed estimates of sediment export at the watershed scale.

3.3.1 Methodology

In the absence of sediment gauge data for the Boughezoul watershed, two complementary approaches were adopted for estimating SDR:

3.3.1.1 Area-Based Empirical SDR Method

An empirical formula adapted for Mediterranean and semi-arid basins was applied, as proposed by Williams and Berndt (1977) and later endorsed by FAO (2006):

$$\mathbf{SDR = 0.472 \times A^{(-0.125)}} \ldots\ldots\ldots\ldots\ldots\ldots\ldots\ldots\ldots\ldots\ldots\ldots \mathbf{(7)}$$

Where:

SDR: Sediment Delivery Ratio (dimensionless)

A: Watershed area (in km²)

For the Boughezoul watershed (A = 2838.48 km²), the calculation yields:

$$\mathbf{SDR \approx 0.472 \times 2838.48^{(-0.125)} \approx 0.17}$$

This implies that approximately 17% of the gross soil loss predicted by RUSLE is expected to reach the watershed outlet, while the remaining 83% is retained within the landscape due to deposition.

3.3.1.2 Slope-Based SDR Estimation (for Spatial Mapping)

To account for spatial variation in sediment connectivity, a slope-dependent empirical SDR approach was also applied, suitable for distributed GIS modeling. This method uses slope as a proxy for transport efficiency and is expressed as:

$$\mathbf{SDR} = \frac{(\mathbf{0.472} \times \sqrt{\boldsymbol{Slope}})}{(\mathbf{1} + \sqrt{\boldsymbol{Slope}})} \ldots\ldots\ldots\ldots\ldots\ldots\ldots\ldots\ldots\ldots\ldots\ldots \mathbf{(8)}$$

Where Slope is the local terrain gradient in degrees. This formula was applied in raster format using the slope layer derived from the ASTER DEM. The resulting SDR map reflects topography-driven variation in sediment delivery efficiency. Steeper slopes are associated with higher SDR values due to their increased capacity to transport sediments downslope with minimal deposition, whereas flatter areas exhibit lower SDR due to longer residence time and trapping potential. This spatial SDR map was later multiplied with the RUSLE soil loss raster to derive the final sediment yield distribution in tons per hectare per year (t/ha/yr).The geoprocessing sequence used to generate the SDR and sediment yield maps is summarized in (Figure 3.12).

Figure 3.12: ArcGIS ModelBuilder workflow for integrating SDR into sediment yield estimation.

The spatial distribution of sediment yield in the Boughezoul watershed, combining RUSLE and SDR results, is presented in (Figure 3.13).

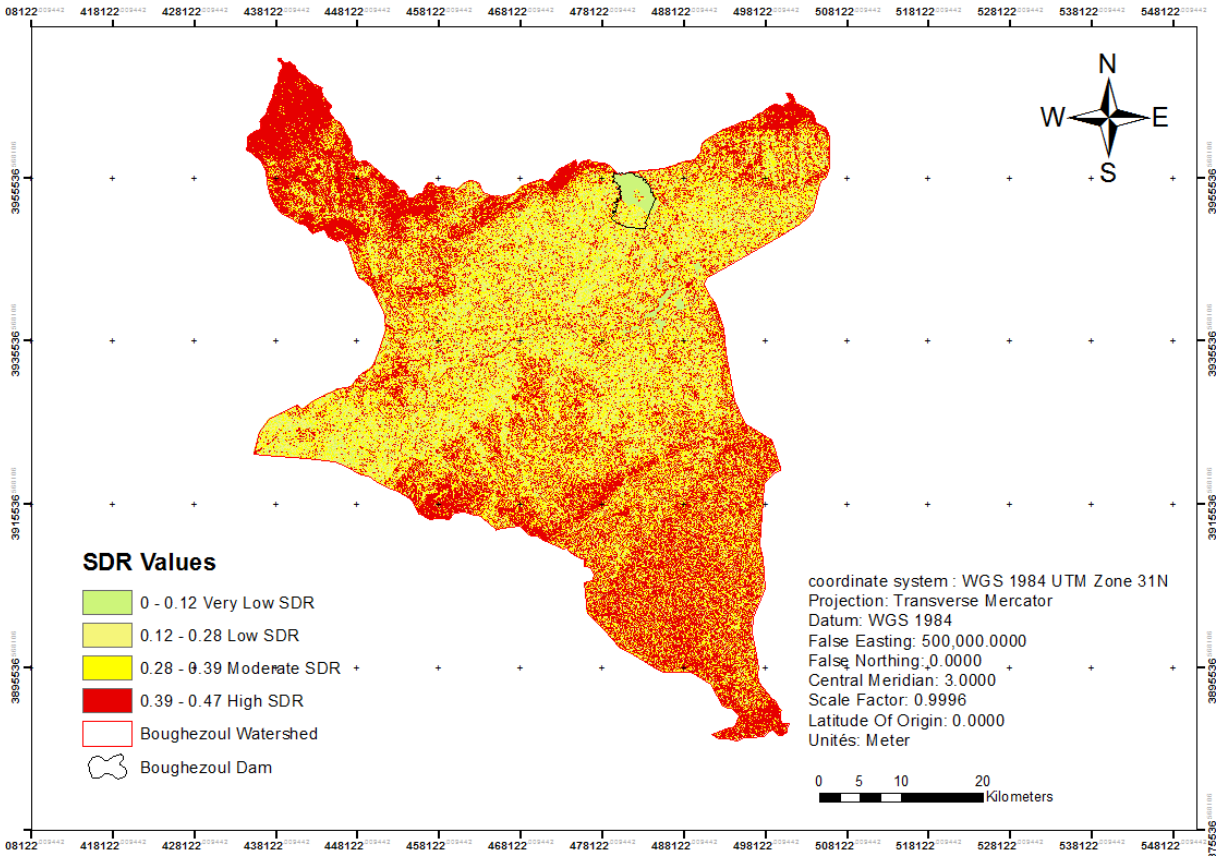

Figure 3.13: Sediment SDR map for the Boughezoul watershed based on RUSLE and SDR integration.

The SDR map quantifies the proportion of eroded soil that is effectively transported from each location to the watershed outlet. It provides insight into the spatial variation of sediment connectivity and the efficiency of sediment transfer, which are critical for assessing downstream siltation and water quality risks.

Four classes of SDR values were identified across the Boughezoul watershed:

Very Low SDR (0 – 0.12): These areas, typically located on flat terrain or in natural depressions, exhibit minimal sediment transport. Due to low slope and reduced runoff energy, most sediments are retained locally, making these zones natural buffers within the watershed.

Low SDR (0.12 – 0.28): Found in regions with gentle slopes and moderate flow accumulation, these areas allow partial sediment movement. While some sediments are delivered downstream, a significant fraction remains trapped within the landscape.

Moderate SDR (0.28 – 0.39): These zones are associated with increased slope and surface runoff. Sediment transport is more effective along these pathways, particularly where topography funnels flow toward drainage lines.

High SDR (0.39 – 0.47): These are critical sediment-export areas, typically on steep slopes or headwater zones. With high flow velocity and limited deposition potential, these locations contribute significantly to downstream sediment yield and are key targets for erosion control and sediment management.

This SDR map, when combined with RUSLE soil loss estimates, enhances the spatial accuracy of sediment yield modeling by incorporating topography-driven sediment transport efficiency.

3.4 Terrain and Hydrologic Indices

Terrain and hydrologic indices are essential components in spatial soil erosion modeling. They help characterize flow accumulation, runoff energy, and terrain structure, all of which influence the detachment, transport, and deposition of sediments (Zhuang et al., 2021; Kinnell, 2016). In this study, several indices were computed using the ASTER DEM and GIS-based hydrological tools to analyze the Boughezoul watershed.

3.4.1 Stream Power Index (SPI)

The Stream Power Index (SPI) quantifies the erosive power of concentrated overland flow and is computed as follows:

$$\mathbf{SPI = FlowAccumulation \times \tan(SlopeRadians)} \quad \text{.....(8)}$$

Where: FlowAccumulation is the specific catchment area, and β is the slope in radians.

High SPI values are typically associated with areas of high erosive energy, such as gullies and convergent slopes (Moore et al., 1991; Wang et al., 2019). It was generated using ArcGIS, based on slope and flow accumulation layers derived from the DEM.

To illustrate the spatial distribution of erosive energy within the Boughezoul watershed, the map below (Figure 3.14) displays the SPI values, categorized into different levels of erosion potential, ranging from low to high erosive energy.

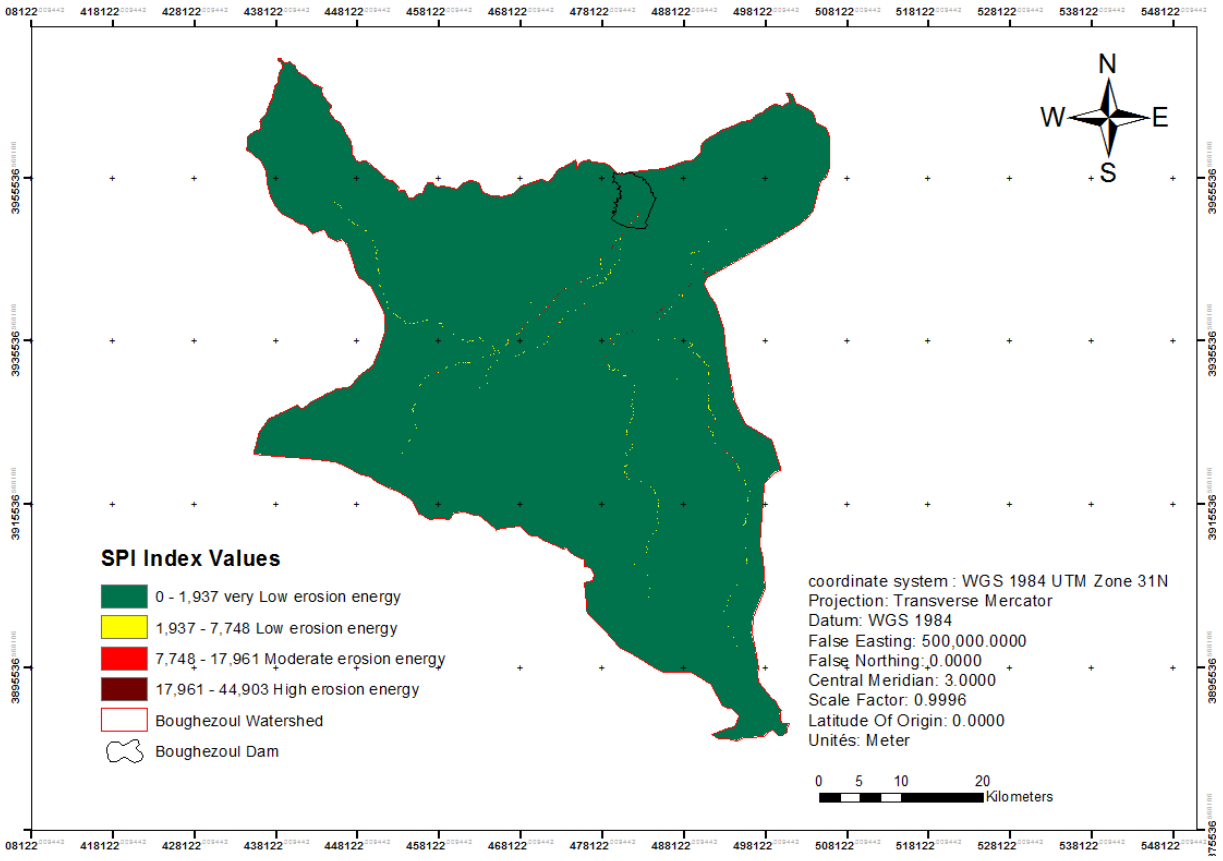

Figure 3.14: Stream Power Index (SPI) Map of the Boughezoul Watershed.

As illustrated in Figure .314, the SPI values across the Boughezoul watershed were classified into four distinct categories of erosion potential:

Very low (0 – 1,937): These areas are typically flat or have minimal flow accumulation, indicating limited erosive force.

Low (1,937 – 7,748): Transitional slopes with moderate accumulation; erosion is possible but controlled.

Moderate (7,748 – 17,961): Concentrated flow paths with increasing erosive power, often found around tributary convergence.

High (17,961 – 44,903): Strongly sloped areas with large upstream contributions, highly susceptible to rill and gully formation.

The spatial pattern shows that high SPI values align with drainage lines and steep terrain in the southern and northeastern regions, reflecting zones of potential hydrodynamic erosion (Yang et al., 2021).

3.4.2 Sediment Deposition Index (SDI)

The Sediment Deposition Index (SDI) is the inverse of the SPI and identifies areas where sediment is likely to deposit:

$$SDR = \frac{1}{SPI} \quad \text{..... (9)}$$

It was derived by inverting the SPI raster using conditional logic in Raster Calculator (Moore et al., 1991). Figure 3.15 presents the Sediment Deposition Index (SDI) across the Boughezoul watershed.

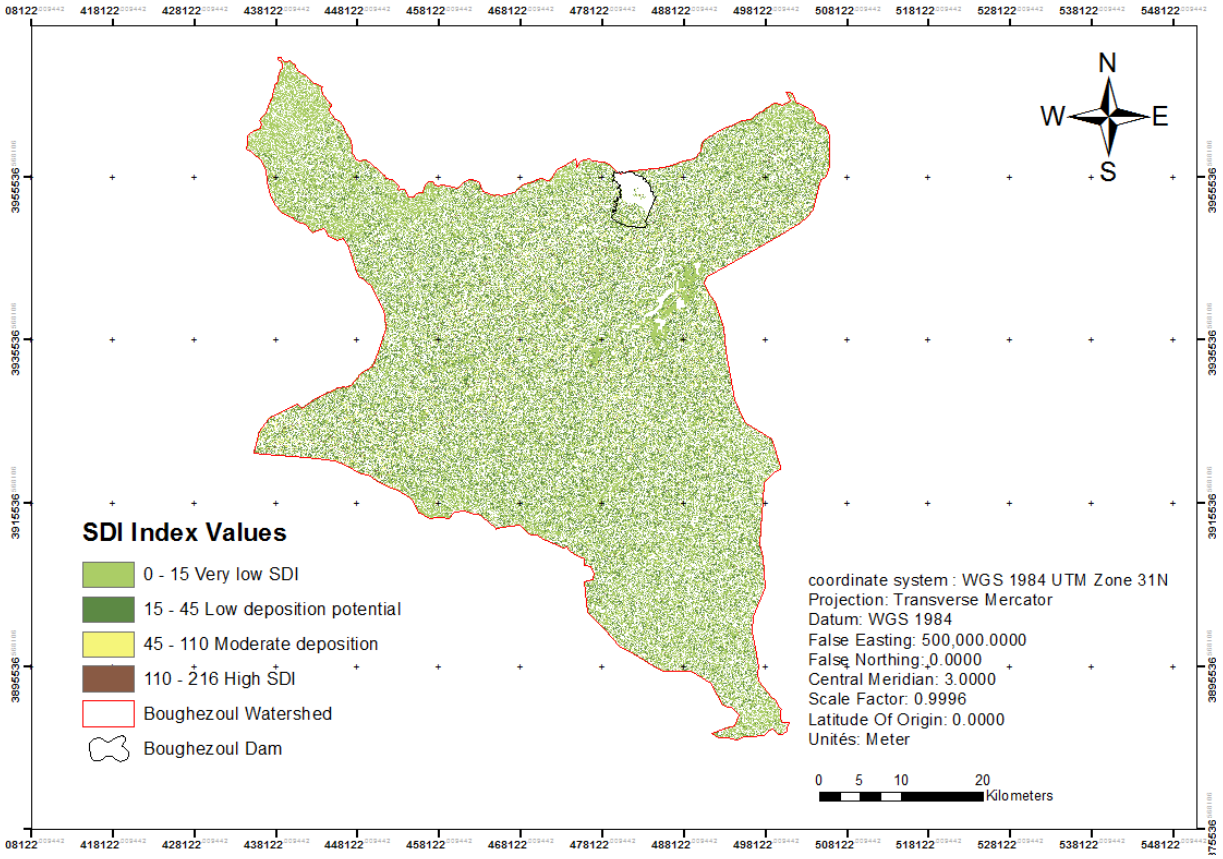

Figure 3.15: Sediment Deposition Index (SDI) Map of the Boughezoul Watershed.

The SDI delineates four distinct zones prone to sedimentation:

Very low SDI (0 – 15): Active erosion zones where sediment is less likely to settle.

Low deposition potential (15 – 45): Found on moderate slopes where partial sediment retention may occur.

Moderate deposition (45 – 110): Footslopes and concave topographies where runoff velocity decreases.

High deposition (110 – 216): Typically found in flat downstream areas, indicating sediment traps or depositional basins.

SDI visualization confirms deposition downstream from high SPI zones, validating the flow-energy dynamics of the catchment (Shang et al., 2021).

3.3.3 Compound Topographic Index (CTI)

The Compound Topographic Index (CTI), also known as the Topographic Wetness Index (TWI), combines upslope contributing area and slope to model soil saturation. The CTI is calculated using the following equation:

$$\mathbf{CTI} = \frac{ln(FlowAccum)}{tan(SlopeRadians)} \quad \text{..... (10)}$$

The Compound Topographic Index (CTI) helps identify areas that are more likely to be saturated, where sediment deposition tends to occur (Beven& Kirkby, 1979; Lei et al., 2020). Figure 3.16 below illustrates the spatial distribution of the Compound Topographic Index (CTI) across the Boughezoul watershed.

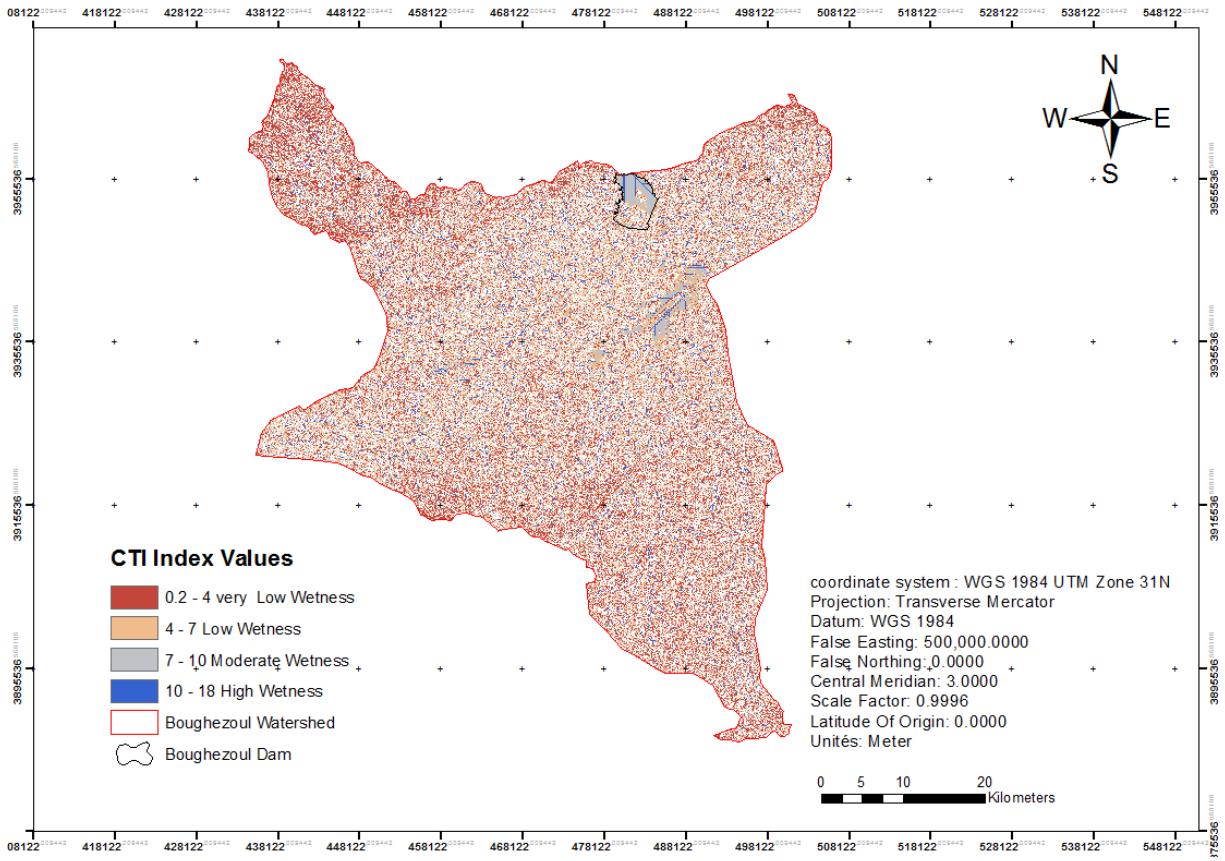

Figure 3.16: Compound Topographic Index (CTI) Map of the Boughezoul Watershed

The map above illustrates four classes of moisture:

Very low wetness (0.2 – 4): Dry ridges or convex slopes with rapid drainage.

Low wetness (4 – 7): Moderately elevated terrain with partial saturation.

Moderate wetness (7 – 10): Lower slopes or toe-slope areas where water begins to accumulate.

High wetness (10 – 18): Valley bottoms and flat areas prone to saturation and potential sedimentation.

The CTI distribution overlaps well with SDI zones, confirming that saturated areas favor sediment deposition (Martinez-Carreras et al., 2020).

3.4.3 Terrain Ruggedness Index (TRI)

The Terrain Ruggedness Index (TRI) quantifies terrain variability by calculating the elevation difference between a central cell and its surrounding neighbors. This isexpressed mathematically as follows:

$$\textbf{TRI} = \sqrt{\boldsymbol{\Sigma}(\boldsymbol{z\_i} - \boldsymbol{z\_mean})^2} \quad \textbf{(12)}$$

Where:

- **z_i** = elevation value of the i neighboring cell around the central cell,
- **z_mean** = mean elevation of the central cell and its neighboring cells**,**
- TRI = terrain ruggedness index value assigned to the central cell.

This index highlights unstable terrain areas that are prone to mechanical erosion and was computed using focal statistics in ArcGIS (Riley et al., 1999; Zhang et al., 2017).

Figure 3.17 below illustrates the Terrain Ruggedness Index (TRI) across the Boughezoul watershed, with areas classified based on their degree of ruggedness.

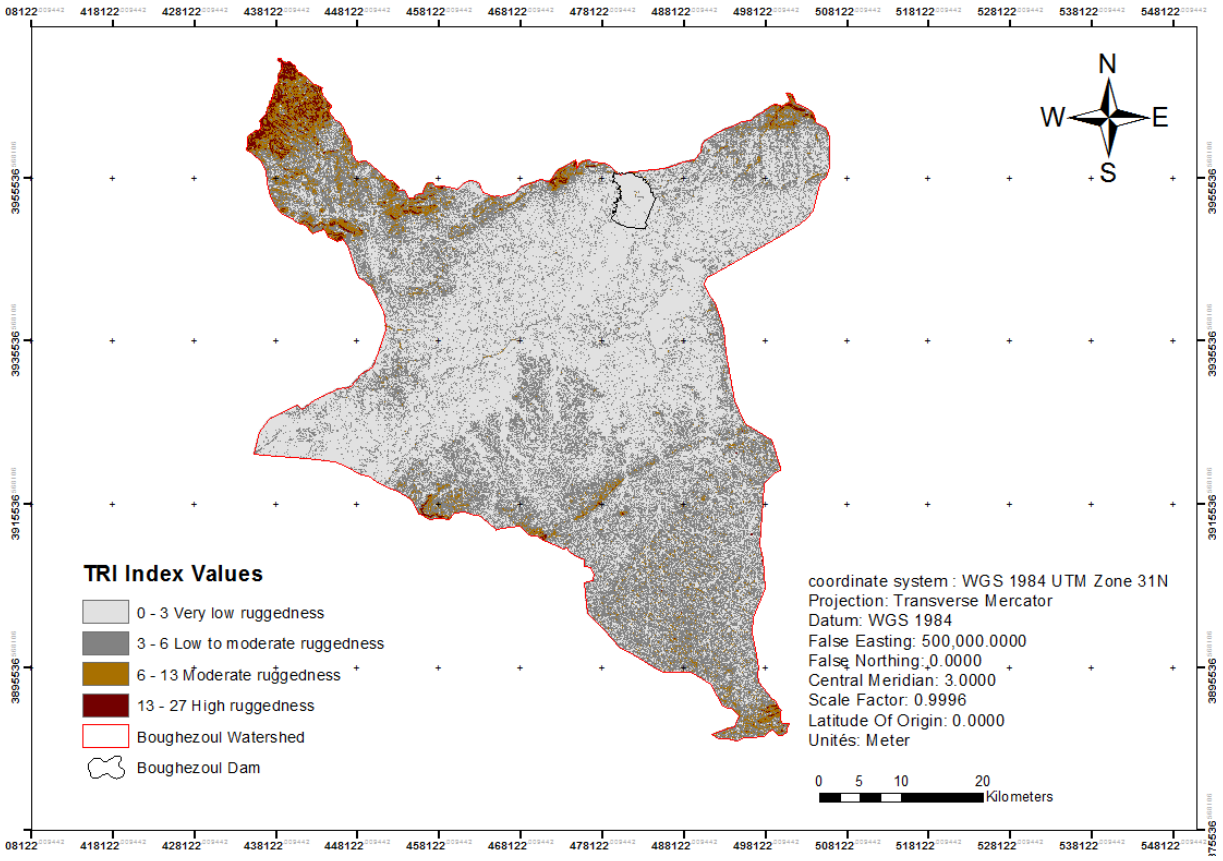

Figure 3.17: Topographic Ruggedness Index (TRI) Map of the Boughezoul Watershed.

The TRI evaluates surface variability and slope heterogeneity, with four classification categories identified:

Very low ruggedness (0 – 3): Homogeneous plains or valley bottoms with stable morphology.

Low to moderate (3 – 6): Gently undulating terrain with moderate relief transitions.

Moderate ruggedness (6 – 13): Sloped areas with noticeable elevation differences.

High ruggedness (13 – 27): Sharp elevation contrasts, often on hilltops or dissected terrain.

This index identifies the northern part of the watershed as topographically unstable, with possible implications for landslides or mechanical erosion (Fu et al., 2021).

3.5 Generation of Indices in ArcGIS

All indices were derived using the Spatial Analyst tools in ArcGIS 10.4. DEM preprocessing included sink filling, slope calculation, and flow direction modeling. Raster Calculator and Focal Statistics were used for mathematical operations. Each index raster was resampled to 30 meters and clipped to the Boughezoul watershed boundary.

3.6 Conclusion

This chapter outlined the integrated methodological approach used to assess soil erosion and sediment yield in the Boughezoul watershed. By combining the RUSLE model with GIS-based terrain analysis and SDR estimation, the study harnessed empirical modeling within a spatially explicit framework adapted to data-scarce, semi-arid environments.

Key model factors R, K, LS, C, and P were derived from global and regional datasets, processed through ArcGIS, and calibrated to reflect local geomorphological and climatic conditions. Supplementary indices such as SPI, CTI, SDI, and TRI enhanced the spatial resolution of erosion risk assessment, while SDR integration allowed for a more realistic estimation of sediment delivery.Altogether, the approach ensures both methodological rigor and operational feasibility, enabling targeted erosion mapping and supporting effective land management planning.

Chapter 4

Results and Discussion

Chapter 4 Results and Discussion

4.1 Spatial Analysis of RUSLE Erosion Factors

Each of the five RUSLE input factors (R, K, LS, C, and P) was calculated as a raster layer and subsequently classified into erosion risk categories. Their spatial distribution illustrates the heterogeneity of climatic, pedological, topographic, and land management conditions across the Boughezoul watershed.

4.1.1 RUSLE Erosion Rate Map

The RUSLE-based soil erosion map illustrates the spatial distribution of average annual soil loss (t/ha/yr) across the Boughezoul watershed. This final output integrates the combined effects of the five RUSLE input factors (R, K, LS, C, and P), and serves as a critical layer for assessing land degradation and guiding targeted intervention strategies (Alewell et al., 2019). The conceptual diagram (Figure 4.1) illustrates the structure of the RUSLE model and the contribution of each input factor to soil loss estimation. This model was implemented in a GIS environment (ArcMap), and the geospatial processing resulted in a thematic erosion risk map of the Boughezoul watershed (Figure 4.2).

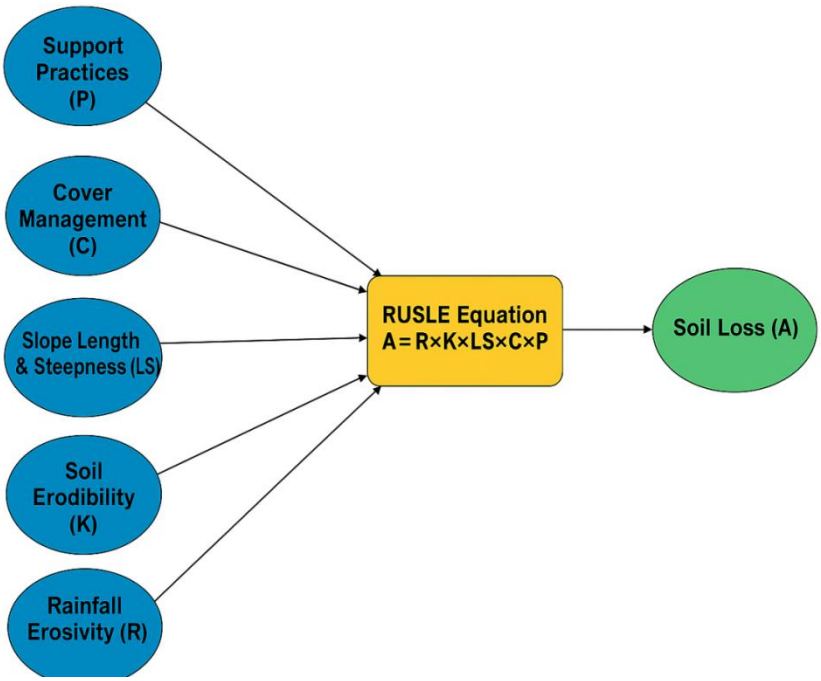

Figure 4.1: Conceptual Structure of the RUSLE Model

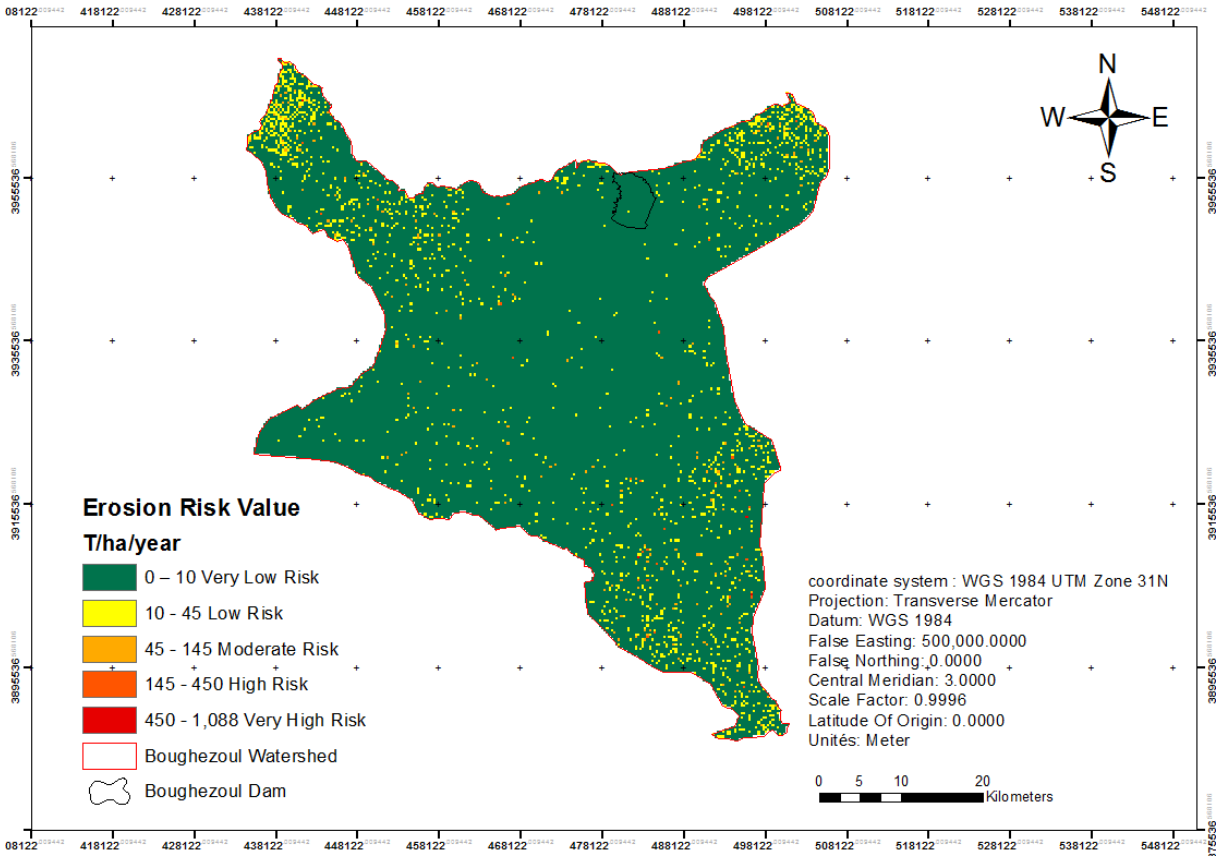

Figure 4.2: RUSLE Erosion Risk Map of the Boughezoul Watershed.

The erosion risk map (Figure 4.2) was classified into five categories using the natural breaks (Jenks) method to emphasize spatial differences in erosion intensity across the Boughezoul watershed:

Very Low Erosion Risk class (0 – 10 t/ha/yr)

This category is primarily associated with flat plains, riverbeds, and areas characterized by dense vegetation and minimal slope. Soils in these regions tend to remain stable, as erosive forces are either naturally mitigated or effectively managed through appropriate land use practices.

Low Erosion Risk class (10 – 45 t/ha/yr)

This class corresponds to gently sloping cultivated lands where vegetation cover is maintained for most of the year. Although erosion processes are active in these areas, they remain within sustainable limits under current land management practices. However, poor agricultural management could lead to a rapid escalation in erosion severity.

Moderate Erosion Risk class (45 – 145 t/ha/yr)

These areas are typically located on mid-slopes and are often associated with agricultural use, partial vegetation cover, and moderate to high LS factor values. Visible signs of erosion, such as sheet and rill formation, are common during rainfall events. These zones should be considered a moderate priority in soil conservation planning.

High Erosion Risk class (145 – 450 t/ha/yr)

This category includes steeply sloped cultivated lands, degraded rangelands, and areas lacking effective erosion control measures. High runoff and susceptible soil conditions significantly accelerate land degradation, making these zones a high priority for targeted conservation interventions.

Very High Erosion Risk areas (450 – 1,088 t/ha/yr)

These zones are concentrated on steep escarpments and badlands characterized by sparse vegetation cover and highly erodible soils. They exhibit severe erosion features, including deep rills and gullies, and are classified as critical areas requiring urgent intervention through reforestation, structural conservation measures, and long-term land use planning.

This erosion risk map serves as a foundational tool for watershed management planning. By identifying the most erosion-prone areas, it enables targeted interventions and facilitates efficient resource allocation for soil and water conservation efforts.

4.2. Modeling Sediment Yield Using RUSLE and Sediment Delivery Ratio

This section presents the modeling and interpretation of the Sediment Delivery Ratio (SDR) and Sediment Yield, both derived from the integration of Revised Universal Soil Loss Equation (RUSLE) outputs with watershed-specific topographic attributes. These two parameters are critical for quantifying the proportion of eroded soil that is effectively transported and deposited downstream. A rasterized SDR layer was multiplied by the soil loss raster generated from the RUSLE model to produce the final Sediment Yield Map, expressed in tons per hectare per year (t/ha/yr). This map offers a spatially explicit and more realistic depiction of sediment export across the watershed, highlighting sediment source areas, zones of internal deposition, and erosion hotspots connected to the stream network.

4.2.1. Sediment Yield Map

To generate the final spatial sediment yield map, a uniform Sediment Delivery Ratio (SDR) coefficient of 0.17 was applied to the RUSLE output raster using the Raster Calculator tool in ArcGIS. The computation was performed as follows:

$$\textbf{SedimentYield} = \textbf{RUSLE} * \textbf{SDR} \quad \textbf{(13)}$$

The resulting raster effectively captures the spatial heterogeneity of sediment delivery within the Boughezoul watershed. It distinctly delineates areas exhibiting high sediment export potential from those dominated by sediment retention processes. Such spatial differentiation provides critical insights for the formulation of site-specific soil and water conservation strategies aimed at mitigating land degradation and enhancing watershed resilience. Figures 4.3 and Figure 4.4 provide a visual representation of the applied methodology and the spatial distribution of sediment yield across the study area.

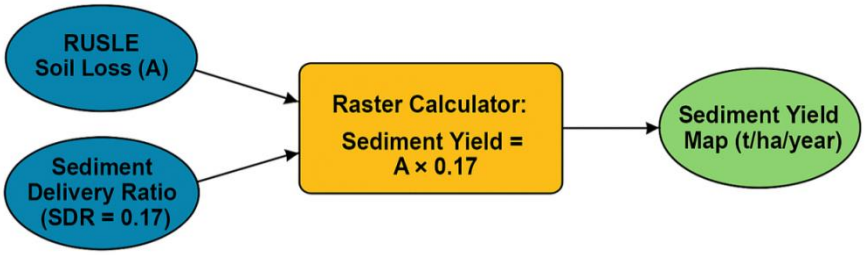

Figure 4.3: Conceptual Structure of the Sediment Yield.

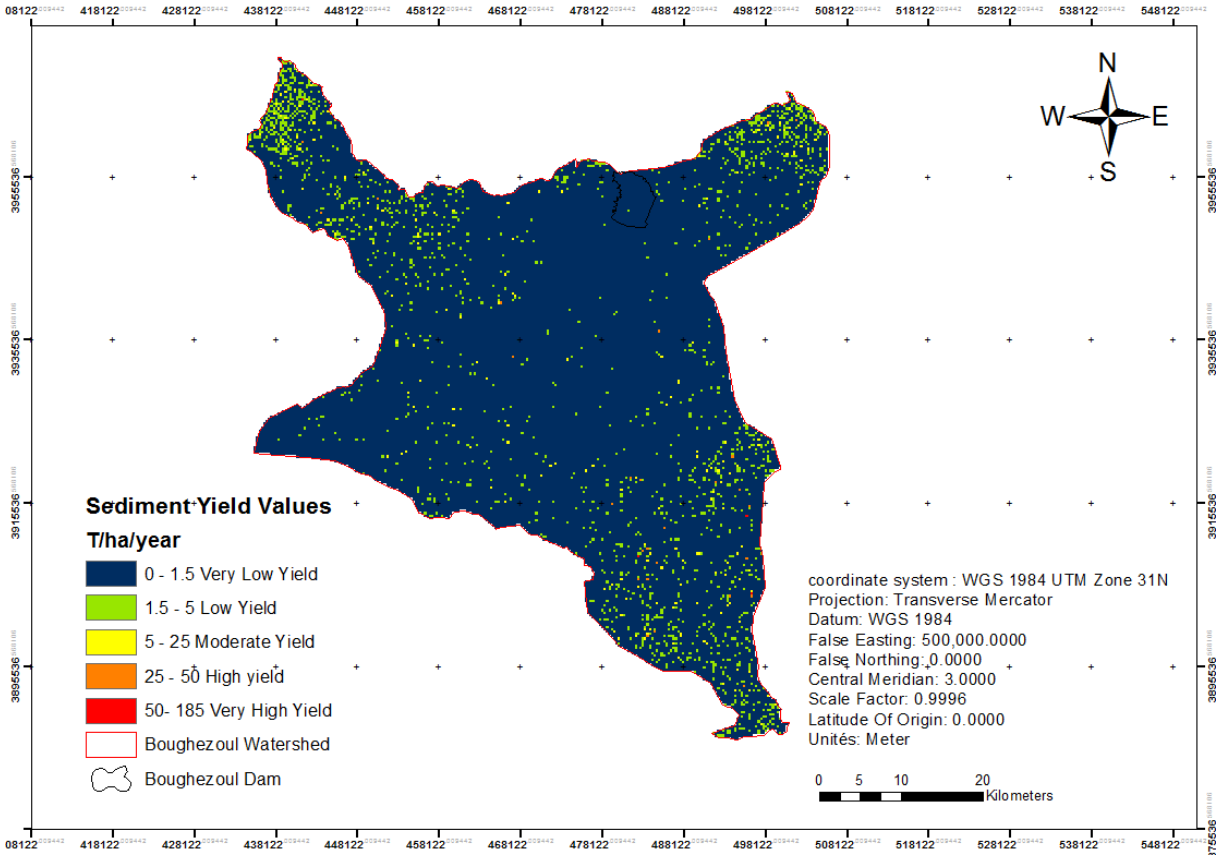

Figure 4.4: Sediment Yield Map of the Boughezoul Watershed.

Further analysis of the sediment yield map presented in Figure 4.4 highlights five distinct sediment yield classes:

Very Low Yield (0 – 1.5 t/ha/yr): These areas are primarily located in well-vegetated valleys, flat depositional zones, and agricultural fields with effective conservation practices. They act as natural sediment sinks, where most of the eroded material is retained onsite and does not contribute to downstream sediment transport.

Low Yield (1.5 – 5 t/ha/yr): Distributed across mid-slope terraces and gentle footslopes, these areas exhibit active but moderated erosion. Sediment is partially re-deposited or retained before reaching major drainage pathways, serving as important buffer zones in sediment dynamics.

Moderate Yield (5 – 25 t/ha/yr): This class includes cultivated lands with moderate slopes, scattered bare patches, and average SDR values. These areas are particularly sensitive to seasonal runoff events and can contribute significantly to downstream siltation, especially during heavy rainfall.

High Yield (25 – 50 t/ha/yr): Found mainly on sloped agricultural parcels with inadequate ground cover and weak protection (low P-factor values), often associated with high LS or SPI indices. These zones act as major sediment source areas and have a substantial impact on sediment delivery to the river network.

Very High Yield (50 – 185 t/ha/yr): Localized in steep, degraded slopes, poorly managed rangelands, and active gully systems. These represent critical sediment hotspots with extremely high erosion and export rates, particularly during storm events. Immediate and site-specific conservation measures such as terracing, revegetation, or the installation of hydrological barriersare necessary to stabilize these zones.

Overall, the sediment yield map complements the RUSLE model by providing not only an estimate of erosion intensity but also a spatial perspective on sediment export potential. This dual-layered insight supports the development of targeted, spatially explicit strategies for soil and water conservation, prioritizing high-risk areas for intervention.

4.3. Final Terrain–Hydrologic Index Map

The Final Terrain–Hydrologic Index Map provides an integrated spatial representation of the terrain and hydrologic factors that influence erosion susceptibility within the Boughezoul watershed. This map synthesizes key topographic indices namely, the Stream Power Index (SPI)**,** Slope-Dependent Index (SDI)**,** Terrain Ruggedness Index (TRI)**,** and Compound Topographic Index (CTI) into a normalized raster format. Such integration enhances the identification and spatial delineation of erosion-prone areas by capturing terrain-driven

hydrologic responses. The methodological workflow employed to construct the Final Terrain–Hydrologic Index Map is illustrated in Figure 4.5**,** which outlines the steps involved in integrating the normalized topographic indicators. The resulting spatial distribution of these indices throughout the Boughezoul watershed is presented in Figure 4.6, offering insights into the terrain's influence on hydrological processes and erosion potential.

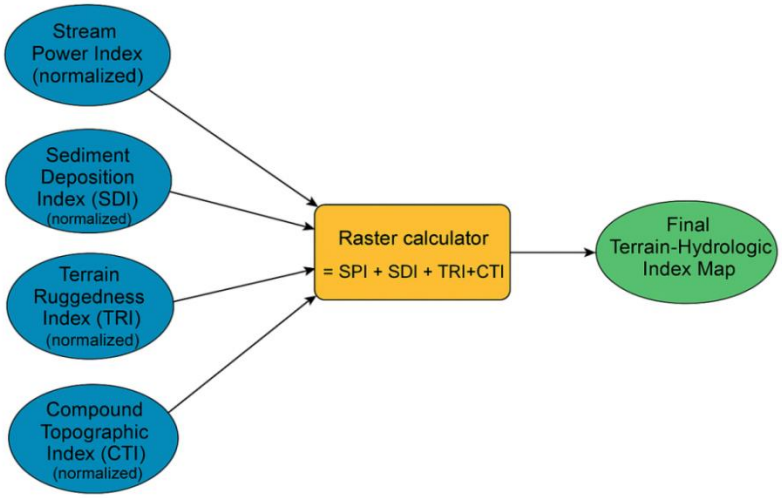

Figure 4.5: Workflow for generating the final terrain–hydrologic index map using normalized topographic indicators.

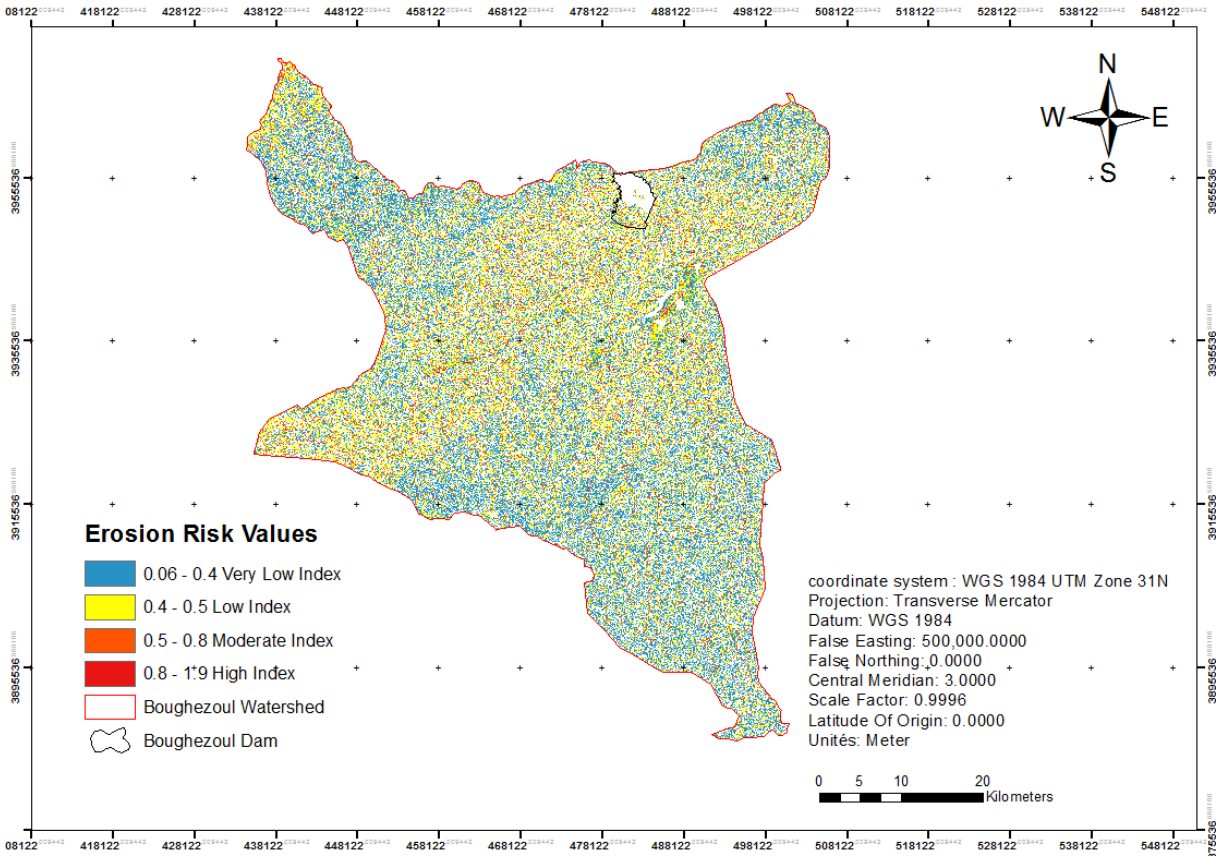

Figure 4.6: Hydrological and Topographic indices Map of the Boughezoul Watershed.

The index values were reclassified into four categories using natural breaks, providing insight into terrain-induced erosion dynamics:

Very Low Index (0.06 – 0.4): These zones are primarily found in flat upstream basins, low-gradient terraces, and well-vegetated areas. Characterized by minimal slope energy and low hydrological convergence, they exhibit stable surface conditions and act as effective sediment retention areas.

Low Index (0.4 – 0.5): Distributed across gently undulating cultivated lands and mid-slope depositional areas, these regions exhibit moderate terrain influence. While not critical in terms of detachment or delivery, these zones may become vulnerable under intensified land use or reduced vegetative cover.

Moderate Index (0.5 – 0.8): Often located on hillslopes with moderate steepness and partial vegetation loss, these zones show increasing signs of hydrologic connectivity and flow accumulation. Their terrain configuration enhances runoff concentration and slope instability, making them priority areas for preventive conservation practices such as buffer strips or mulching.

High Index (0.8 – 1.9): These represent the most erosion-susceptible terrains, generally located on dissected slopes, gully heads, and flow convergence zones. With strong runoff potential and limited vegetation, these critical zones are prone to severe erosion and sediment transport. Immediate intervention is required such as contour trenching, check dams, or reforestation to stabilize the terrain and reduce downstream impacts.

This terrain–hydrologic index complements the RUSLE and SDR outputs by capturing topographic predisposition to both detachment and delivery. It enhances the understanding of spatial erosion patterns and supports informed decision-making in watershed management by identifying terrain-controlled erosion hotspots.

4.3. Comparative Integration and Validation

4.3.1. Spatial Correlation: Intermediate Maps and Final Erosion Risk Index

The comparison between intermediate spatial models namely the RUSLE erosion risk map, the sediment yield output, and the terrain–hydrologic index reveals a coherent yet complementary distribution of erosion vulnerability across the Boughezoul watershed. Each map contributes a specific dimension of the erosion process:

RUSLE (t/ha/year) highlights zones of high soil detachment potential, particularly in cultivated hillslopes, bare lands, and areas with poor land management. Its highest values are concentrated along steep agricultural gradients and degraded grazing zones.

Sediment Yield (t/ha/year) refines the detachment information by incorporating sediment transport potential. High sediment yield zones overlap with high RUSLE zones but are more spatially constrained to slope breaks, convex hills, and drainage-convergent sectors where sediment delivery is more efficient.

Final Terrain–Hydrologic Index characterizes terrain response to hydrological forcing, highlighting topographically sensitive areas such as dissected escarpments, gully networks, and convergence zones. This index reveals critical areas where slope, drainage accumulation, and surface roughness amplify erosion processes.

The overlay and cross-comparison of these three layers underpin the construction of the Final Erosion Risk Map**,** which aggregates the combined effects of detachment, delivery, and terrain predisposition. Zones with consistently high values across all three indicators such as the central ridges, southern escarpments, and stream-adjacent gullies are confirmed as erosion hotspots. These are not only prone to soil loss but also actively contribute to sediment connectivity and downstream degradation.

This spatial triangulation validates the reliability of the composite approach: while RUSLE identifies where erosion begins, sediment yield estimates where it is likely to move, and the terrain index reveals how the landscape facilitates or impedes this process. The final composite map thus reflects a synthesized, high-resolution erosion risk assessment that enables precise, evidence-based intervention planning.

4.4. Final Erosion Risk Map Interpretation (Composite Map)

The Final Erosion Risk Map represents a comprehensive spatial synthesis of erosion vulnerability across the Boughezoul watershed. It results from the integration of modeled erosion outputs with topographic indices that characterize terrain-driven susceptibility to runoff and sediment transport. This composite layer accounts not only for soil detachment and delivery dynamics but also for the amplifying effects of slope, flow accumulation, and surface roughness providing a refined spatial understanding of erosion intensity.

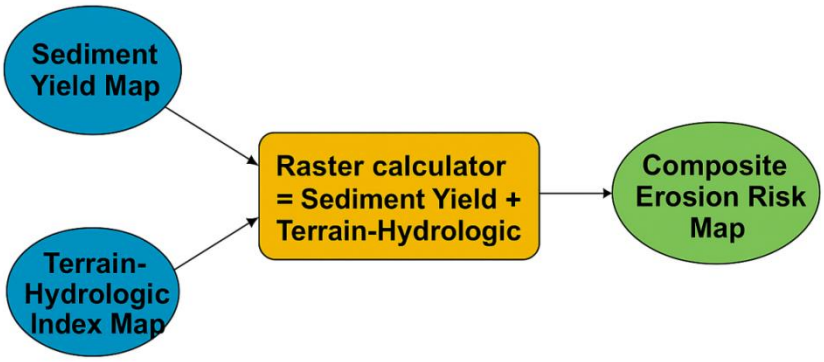

Figure 4.7: Workflow for Generating the Composite Erosion Risk Map from Sediment Yield and Terrain–Hydrologic Indices

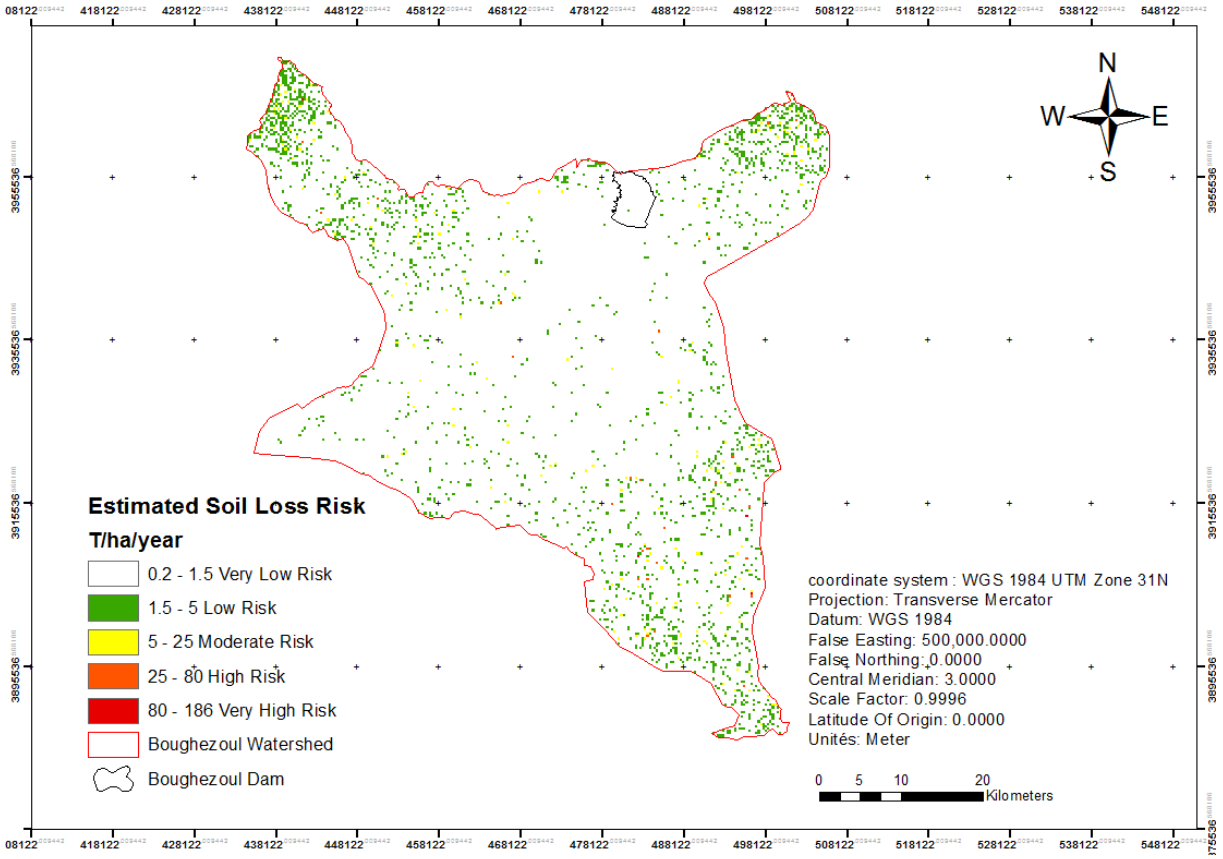

Figure 4.8: Composite Erosion Risk Map of the Boughezoul Watershed.

The composite erosion risk map highlights five distinct classes of vulnerability, reflecting a spatial gradient in erosion severity across the watershed:

Very Low Risk (0.2 – 1.5 t/ha/year): This category includes upstream flatlands, low-lying depressions, and densely vegetated zones where runoff energy is minimal. These areas demonstrate stable soil conditions and high sediment retention capacity, resulting in negligible susceptibility to erosion under current land use and climatic conditions.

Low Risk (1.5 – 5 t/ha/year): Located on gentle slopes and cultivated lands with partial vegetative cover and stable terrain. These areas contribute marginally to overall sediment movement but could become more vulnerable with land-use intensification.

Moderate Risk (5 – 25 t/ha/year): Associated with mid-slope zones where erosive processes are active, especially during seasonal rainfall. Terrain characteristics and moderate flow accumulation increase the risk of sediment mobilization. These areas are priority zones for preventive land management.

High Risk (25 – 80 t/ha/year): Concentrated on steep, poorly managed slopes with limited vegetation and elevated topographic indices. These zones exhibit both high erosion and strong connectivity to drainage networks, posing a serious risk of sediment export and land degradation.

Very High Risk (80 – 186 t/ha/year): Corresponds to critical hotspots located on dissected terrain, gully systems, and escarpments with intense runoff concentration. These sectors combine maximum detachment and delivery potential with minimal natural protection, making them top priorities for structural erosion control and ecological restoration.

This final risk map offers a powerful decision-support tool for erosion mitigation planning. By identifying zones where topographic drivers exacerbate sediment movement, it helps prioritize conservation interventions with greater spatial precision and strategic value.

4.5. Critical Zones for Erosion Control

The final erosion risk map, developed through the integration of sediment yield and terrain hydrologic indices, highlights several critical zones requiring immediate attention for effective soil and water conservation.

Steep central and southern slopesdemonstrate very high erosion risk due to intense runoff, minimal vegetation, and poor land management. These areas require urgent structural interventions such as check dams, terracing, and gully rehabilitation to reduce soil detachment and improve retention (Renard et al., 1997; Liu et al., 2018).

Hill slope valley transitions and flow convergence zones in the mid-watershed combine moderate sediment production with high topographic delivery potential. These zones are ideal for implementing buffer strips, grassed waterways, or sediment traps, which can reduce sediment export by up to 100% depending on vegetation type and width (Williams & King, 2014; Schulte-Moore et al., 2012).

Riparian corridors and gully headstypically concave and sparsely vegetated are hotspots for both erosion and sediment transport. Restoration strategies such as riparian buffer planting, reforestation, and bioengineering have proven effective in stabilizing stream banks and limiting channel erosion (Shrestha et al., 2020; García-Ruiz et al., 2013).

This spatial prioritization balances source control (erosion initiation areas) with deliveryinterruption (sediment transfer zones), supporting highly targeted and cost-effective erosion mitigation (Borrelli et al., 2017).

4.6. Implications for Watershed Management

The integration of erosion modeling, sediment delivery assessment, and terrain–hydrologic analysis into a unified erosion risk map provides a robust framework for watershed-scale management. This spatially explicit tool enables targeted intervention by delineating zones according to both erosion severity and sediment transport potential. In areas classified as low to moderate risk, where slopes are gentle and vegetation cover remains partially intact preventive land management practices are most suitable. Techniques such as conservation tillage, mulching, crop rotation, and agro forestry can effectively maintain soil structure, enhance infiltration, and reduce surface runoff (Morgan, 2005; Nyssen et al., 2004). These approaches aim to preserve existing land productivity while mitigating future degradation.

For zones characterized by moderate to high erosion risk, particularly those with flow accumulation and slope convergence, require mitigative measures to intercept sediment before it enters the main drainage network. Contour farming, vegetated buffer strips, and grassed waterways have demonstrated efficacy in reducing sediment transport and stabilizing micro-topographical features without requiring extensive structural modifications (Williams & King, 2014; Schulte-Moore et al., 2012).In contrast, areas identified as very high risk, such as degraded steep slopes and actively eroding gullies necessitate intensive restorative interventions. These include reforestation, terracing, gully rehabilitation, and bioengineering techniques aimed at reestablishing vegetative cover, reducing slope instability, and restoring hydrological balance (Shrestha etal., 2020; Nearing et al., 2017). Such efforts are resource-intensive but critical to reversing severe land degradation and curbing downstream sedimentation.

By operational zing the erosion risk map, decision-makers can allocate financial and technical resources with greater precision, focusing on areas with the highest intervention payoff. Moreover, incorporating sediment connectivity into the planning process enhances the model's predictive capacity, supporting proactive and sustainable land-use planning (Prasuhn et al., 2020).

4.7 Comparison with Previous Studies on the Boughezoul Watershed

Table 4.1 below provides a comparative overview of key findings from previous studies conducted on the Boughezoul watershed, particularly the work by Remini et al. (2015), alongside the current study. While earlier research primarily focused on reservoir sedimentation through bathymetric surveys, the present study employs a more comprehensive modeling framework that integrates RUSLE, Sediment Delivery Ratio (SDR), and terrain–hydrologic indices. This approach not only estimates soil loss but also identifies spatial erosion risk patterns and sediment connectivity across the watershed. The table highlights the evolution of methodologies and underlines the added value of integrating multiple spatial and hydrological indicators in modern erosion assessment.

Table 4.1: Comparative Summary of Erosion Assessment Studies Conducted in the Boughezoul Watershed

Study	Methodology	Key Findings	Notable Differences
Remini et al. (2015) [Remini et al., Journal of Water and Land Development]	Bathymetric surveys (1986 & 2005)	Estimated average annual silting rate of 0.67 million m^3/year; 70% reservoir capacity loss by 2011.	Focused on sedimentation rates without modeling erosion processes.
This Study (2025)	RUSLE, SDR, Terrain–Hydrologic Index	Integrated modeling approach estimating soil loss and sediment yield; identified critical erosion zones.	Combines multiple models for a comprehensive erosion risk assessment.

4.8 Conclusion

This chapter presented an integrated spatial analysis of soil erosion and sediment dynamics in the Boughezoul watershed, using the RUSLE model enhanced by terrain–hydrological indices and sediment delivery modeling. The results revealed significant spatial variability in erosion intensity and sediment yield, largely influenced by topography, land cover, and rainfall erosivity. Critical erosion hotspots were identified along steep slopes, degraded rangelands, and gully-prone zones, where detachment and sediment transport are highly active.

The final erosion risk map, synthesizing RUSLE, SDR, and terrain-based indices, provides a robust decision-support tool for prioritizing conservation efforts. It distinguishes between zones requiring preventive land management and those needing urgent structural interventions. By aligning erosion control strategies with spatially explicit risk patterns, this approach enhances the efficiency and effectiveness of watershed management planning.

General Conclusion

General Conclusion

The Revised Universal Soil Loss Equation (RUSLE) was used as the primary model to estimate average annual soil loss, incorporating five key factors rainfall erosivity (R), soil erodibility (K), topography (LS), land cover (C), and support practices (P) derived from high-resolution datasets adapted to local conditions. Rainfall data were interpolated using the Inverse Distance Weighting (IDW) method over a 10 year period, and soil parameters were calculated from the FAO DSMW database using organic carbon content and granulometry. Land cover classification followed ESA 2020 standards.

To compensate for RUSLE's limitations in representing sediment transport and connectivity, a slope-based Sediment Delivery Ratio (SDR) was applied as a function of local slope gradients. By combining the SDR with RUSLE estimates, a spatially explicit sediment yield map was generated. Complementary terrain and hydrologic indices Stream Power Index (SPI), Terrain Ruggedness Index (TRI), Compound Topographic Index (CTI), and Sediment Deposition Index (SDI) were also calculated from ASTER DEM data to refine the spatial interpretation of erosion processes.

The resulting composite erosion risk map revealed marked spatial variation in erosion intensity across the watershed, with soil loss values ranging from 0.213 to over 186 t/ha/year, categorized into five risk classes. High-risk zones are concentrated on steep, sparsely vegetated slopes in the southern and southeastern parts of the watershed, where losses exceed 80 t/ha/year. The Boughezoul dam lies downstream from several of these critical corridors, underscoring its exposure to sediment accumulation.

Analysis of the SDR indicated that much of the eroded sediment is retained in flatter upstream areas due to low delivery efficiency. However, approximately 17% of total sediment yield is estimated to reach the watershed outlet, particularly from steep, poorly vegetated zones. The integration of soil loss and sediment transport metrics provides a solid basis for identifying both erosion hotspots and key sediment delivery pathways.

The final risk map thus offers a scientifically grounded decision-support tool for prioritizing erosion control and land conservation strategies. By combining empirical modeling, sediment delivery analysis, and terrain-based indices within a GIS framework, this methodology provides valuable insights for hydrologists, land managers, and policymakers. Its adaptable design ensures relevance for other semi-arid regions confronting similar land degradation pressures.

This study demonstrates the effectiveness of spatially integrated approaches for environmental risk assessment. By combining RUSLE, slope-based Sediment Delivery Ratio modeling, and terrain analysis within a GIS framework, it enhances the understanding of erosion dynamics and provides a foundation for sustainable watershed management in Algeria and other semi-arid regions. The integrated methodology developed here can be adapted to other vulnerable regions worldwide, contributing to global efforts in soil conservation and sustainable watershed management.

REFERENCES

Alemu, T., Gebreyesus, B., &Tadele, M. (2025). Assessment of soil erosion using RUSLE and GIS in the Abaya-Chamo basin, Ethiopia. *Modeling Earth Systems and Environment*. https://link.springer.com/article/10.1007/s40808-025-02337-8

Alewell, C., Meusburger, K., Brodowski, S., & Frey, M. (2019). How well can we assess soil erosion with soil organic carbon and 137Cs? *Environmental Research Letters, 14*(8), 084007. https://doi.org/10.1088/1748-9326/ab25f7

Ali, S. A., Khan, A. N., & Sheikh, M. T. (2016). Assessment of terrain indices for soil erosion susceptibility mapping using GIS and remote sensing: A case study of Dabka watershed, India. *Arabian Journal of Geosciences, 9*(3), 1–16. https://doi.org/10.1007/s12517-016-2279-x

Amraoui, M., Derdous, O., &Kettab, A. (2016). Effects of overgrazing on land degradation in semi-arid areas of Algeria: A case study in the Boughezoul basin. *EnvironmentalEarth Sciences, 75*(7), 567. https://doi.org/10.1007/s12665-016-5267-5

ANRH – Agence Nationale des Ressources Hydrauliques. (2021). *Étude hydrogéologique et de modélisation du bassin versant de Boughezoul*. Ministère des Ressources en Eau, Algérie.

Ahmad, M., Ali, M., Khan, A. N., &Zandi, P. (2023). Remote sensing and machine learning integration for RUSLE-based soil erosion mapping. *Catena, 224*, 106560. https://doi.org/10.1016/j.catena.2023.106560

Amraoui, M., Meddi, M., &Meddi, H. (2016). Impact of land use and climate change on soil erosion in a semi-arid region: A case study of the upper Tafna catchment (Algeria). *Arabian Journal of Geosciences, 9*(5), 1–13. https://doi.org/10.1007/s12517-015-2158-2

ANRH. (2021). *Base de données hydrologiques du bassin de Boughezoul*. Agence Nationale des Ressources Hydrauliques, Ministère des Ressources en Eau.

Benrhouma, B., Jebari, S., &Khemiri, N. (2024). Evaluating best management practices for erosion control using SWAT in a semi-arid catchment of Tunisia. *Frontiers in Water, 5*, 1521812. https://www.frontiersin.org/articles/10.3389/frwa.2025.1521812/full

Boix-Fayos, C., de Vente, J., Martínez-Mena, M., Barbero-Sierra, C., & Castillo, V. (2007). The impact of land use on soil erosion in semi-arid environments: A review. *Catena, 68*(2), 93–108. https://www.sciencedirect.com/science/article/abs/pii/S034181620600065X

Benabderrahmane, M., Allache, F., &Guettouche, M. S. (2016). Soil degradation and land vulnerability to erosion in semi-arid Algeria: A case study of Boughezoul. *African Journal of Agricultural Research, 11*(9), 749–758. https://doi.org/10.5897/AJAR2015.10484

Benchetrit, M., Bouarfa, S., & Abdelkader, A. (2018). Modeling soil erosion in Mediterranean and arid environments: Application to Boughezoul, Algeria. *Environmental Monitoring and Assessment, 190*(7), 415. https://doi.org/10.1007/s10661-018-6789-2

Benavidez, R., Jackson, B., Maxwell, D., & Norton, K. (2018). A review of the (Revised) Universal Soil Loss Equation (R/USLE): With a view to increasing its global applicability and

improving soil loss estimates. *Hydrology and Earth System Sciences*, *22*(11), 6059–6086. https://doi.org/10.5194/hess-22-6059-2018

Belhadj, A., Djemai, N., &Hamadache, M. (2013). Lithological and geotechnical characterization of sedimentary formations in central Algeria. *Journal of African Earth Sciences*, *83*, 1–10. https://doi.org/10.1016/j.jafrearsci.2013.01.001

Bessaoud, O., Mebarki, A., &Djebbar, Y. (2018). Climatic variability and land degradation in semi-arid Algeria: The case of the Boughezoul basin. *Environmental Monitoring and Assessment*, *190*(6), 337. https://doi.org/10.1007/s10661-018-6721-9

Borrelli, P., Robinson, D. A., Panagos, P., Lugato, E., Yang, J. E., Alewell, C., &Ballabio, C. (2021). Land use and climate change impacts on global soil erosion by water (2015–2070). *Proceedings of the National Academy of Sciences*, *118*(13), e2016178118. https://doi.org/10.1073/pnas.2016178118

Borselli, L., Cassi, P., &Torri, D. (2008). Prolegomena to sediment and flow connectivity in the landscape: A GIS and field numerical assessment. *Catena*, *75*(3), 268–277. https://doi.org/10.1016/j.catena.2008.07.006

Bouanani, A., Ghenim, A. N., & Remini, B. (2015). Spatial analysis of gully erosion sensitivity in the Boughezoul watershed (Algeria). *Hydrological Sciences Journal*, *60*(11), 1888–1901. https://doi.org/10.1080/02626667.2014.967246

Boudjemaa, A., Benmohamed, A., &Meheni, N. (2021). Integrated hydroclimatic risk assessment for soil erosion in Algerian semi-arid basins. *Journal of Arid Environments*, *191*, 104558. https://doi.org/10.1016/j.jaridenv.2021.104558

Brooks, A. P., & Spencer, J. (2019). Understanding the influence of rainfall thresholds and catchment characteristics on sediment delivery. *Hydrological Processes*, *33*(15), 2215–2229. https://doi.org/10.1002/hyp.13472

Benabderrahmane, M., Touaibia, B., &Bensouiah, R. (2016). Study of soil degradation and salinization in semi-arid irrigated lands: Case of Biskra region, Algeria. *Journal of Water and Land Development*, *31*(1), 29–35. https://doi.org/10.1515/jwld-2016-0004

Benchetrit, R., Bessaoud, O., &Hadeid, M. (2018). L'agriculture en Algérie face aux changements climatiques: Enjeux et perspectives. *Cahiers Agricultures*, *27*(2), Article 24002. https://doi.org/10.1051/cagri/2018010

Belhadj, A., Bouhoun, M. D., & Nait Yahia, A. (2013). Geological and geomorphological influences on hydrological functioning in the Cheliff basin, Algeria. *Journal of African Earth Sciences*, *88*, 80–91. https://doi.org/10.1016/j.jafrearsci.2013.08.002

Bessaoud, O., Hadeid, M., &Benchetrit, R. (2018). Climate variability and the future of agriculture in Algeria: Challenges and adaptation strategies. *Mediterranean Journal of Social Sciences*, *9*(1), 201–212. https://doi.org/10.2478/mjss-2018-0018

Boudjemaa, F., Chettibi, M., &Merad, B. (2021). Spatio-temporal analysis of hydrological extremes in the Cheliff basin. *Environmental Monitoring and Assessment, 193*, Article 187. https://doi.org/10.1007/s10661-021-09031-y

Bouanani, A., Hallouche, B., &Kettab, A. (2015). Assessment of erosion risk in semi-arid environments using RUSLE and GIS: A case study of the Hodna basin, Algeria. *Hydrology Research, 46*(3), 377–386. https://doi.org/10.2166/nh.2014.198

Beven, K. J., & Kirkby, M. J. (1979). A physically based variable contributing area model of basin hydrology. *Hydrological Sciences Bulletin*, 24(1), 43-69. DOI: 10.1080/02626667909491834

Bencheikh-Lehocine, M., Bounoua, L., & Tachi, A. (2020). *Assessment of water erosion in semi-arid regions of Algeria using RUSLE and GIS*. Journal of Water and Land Development, 47(1), 62–71. https://doi.org/10.24425/jwld.2020.134205

Beven, K. J., & Kirkby, M. J. (1979). *A physically based, variable contributing area model of basin hydrology*. Hydrological Sciences Bulletin, 24(1), 43–69. https://doi.org/10.1080/02626667909491834

Borrelli, P., Robinson, D.A., Panagos, P., et al. (2017). An assessment of soil erosion hotspots in Europe. *Science of the Total Environment*, 599–600, 1245–1255. https://doi.org/10.1016/j.scitotenv.2017.04.128

Cherifi, B., Allache, F., &Benslama, M. (2020). Impacts of urban sprawl and road construction on erosion patterns in semi-arid Algeria. *Geocarto International, 35*(10), 1102–1118. https://doi.org/10.1080/10106049.2019.1581572

Cherifi, H., Chenchouni, H., &Bradai, N. (2020). Effects of urban expansion on soil erosion and sediment yield: Case of Boughezoul. *Arabian Journal of Geosciences, 13*(24), Article 1355. https://doi.org/10.1007/s12517-020-06001-w

Chorley, R. J., Schumm, S. A., &Sugden, D. E. (1985). *Geomorphology*. Methuen.

Epple, L., Klik, A., Strauss, P., & Rosner, J. (2022). Performance of process-based models to predict soil erosion in small agricultural catchments—A review. *CATENA, 215*, 106321. https://doi.org/10.1016/j.catena.2022.106321

FAO. (2020). *Harmonized World Soil Database (version 1.2)*. Food and Agriculture Organization of the United Nations. https://www.fao.org/soils-portal/data-hub/soil-maps-and-databases

Fehdi, C., Guettouche, M. S., &Maachou, M. (2017). Effects of surface crusting on runoff and erosion in semi-arid Mediterranean zones: A case study in Algeria. *Catena, 149*, 282–291. https://doi.org/10.1016/j.catena.2016.09.015

FAO. (2020). *Harmonized World Soil Database* (Version 1.2). Food and Agriculture Organization of the United Nations. http://www.fao.org/soils-portal

Fehdi, C., Gharzouli, R., &Chehma, A. (2017). Geological formations and their impact on soil erosion in semi-arid Algeria. *Journal of Arid Environments, 138*, 60–69. https://doi.org/10.1016/j.jaridenv.2016.11.008

Filchev, L., & Kolev, D. (2023). Assessment of soil erosion risk using remote sensing and GIS: A review. *arXiv preprint*. https://arxiv.org/abs/2310.08430

Fu, X., Zuo, D., & Li, H. (2021). Topographic instability and erosion potential in mountainous regions: Insights from the Terrain Ruggedness Index (TRI). *Geomorphology*, 380, 107601. DOI: 10.1016/j.geomorph.2021.107601

Ganasri, B. P., & Ramesh, H. (2016). Assessment of soil erosion by RUSLE model using remote sensing and GIS—A case study of Nethravathi Basin. *Geoscience Frontiers, 7*(6), 953–961. https://doi.org/10.1016/j.gsf.2015.10.007

Gomi, T., Sidle, R. C., & Richardson, J. S. (2002). Understanding processes and downstream linkages of headwater systems. *BioScience, 52*(10), 905–916. https://doi.org/10.1641/0006-3568(2002)052[0905:UPADLO]2.0.CO;2

Guettouche, M. S., Hadji, R., &Boukhemacha, M. A. (2022). Mapping human-induced erosion risk using remote sensing and land use change analysis in the Boughezoul watershed. *Remote Sensing Applications: Society and Environment, 25*, 100705. https://doi.org/10.1016/j.rsase.2022.100705

Guettouche, M. S., &Djellouli, Y. (2022). Modelling the impact of land use changes on soil erosion in Algeria using RUSLE and GIS techniques. *Geocarto International, 37*(5), 1262–1279. https://doi.org/10.1080/10106049.2020.1749585

Gomi, T., Sidle, R. C., & Richardson, J. S. (2002). *Understanding processes and downstream linkages of headwater systems*. BioScience, 52(10), 905–916. https://doi.org/10.1641/0006-3568(2002)052[0905:UPADLO]2.0.CO;2

García-Ruiz, J.M., Lana-Renault, N., & Beguería, S. (2013). Surface wash erosion on mountain farmland in the Central Spanish Pyrenees. *Catena*, 130, 220–231. https://doi.org/10.1016/j.catena.2015.02.020

Hadji, R., Boukhemacha, M. A., &Bouaziz, S. (2020). Soil erosion processes and land degradation risk in the semi-arid region of Algeria. *Environmental Earth Sciences, 79*(13), 324. https://doi.org/10.1007/s12665-020-09055-8

Hamza, N., Bouhata, D., &Boudiaf, B. (2015). Assessment of erosion risk using soil erodibility indicators in the steppe region of Médéa, Algeria. *Catena, 135*, 153–162. https://doi.org/10.1016/j.catena.2015.07.004

Hamelin, S., Allache, F., &Mahé, G. (2020). Land degradation and hydrological impacts in semi-arid Algeria: A case study of the Boughezoul watershed. *Journal of Arid Environments, 174*, 104040. https://doi.org/10.1016/j.jaridenv.2019.104040

Huang, J., Ji, M., Xie, Y., Wang, S., He, Y., & Ran, J. (2020). Global semi-arid climate change over the past 60 years. *Climate Dynamics*, *54*(1), 327–346. https://doi.org/10.1007/s00382-019-05000-4

Hilman Rojak, *"Rill Erosion Definition – Earth Science"*, The Earth Images Revimage.Org, posted February 28, 2019

Hadji, R., Bouhoun, M. D., & Baghdadi, M. (2020). Assessment of soil erosion hazard using GIS and RUSLE model in North Algeria: A case study of Oued Righ region. *Sustainability*, *12*(12), 5035. https://doi.org/10.3390/su12125035

Hamelin, S., Kadi, M., &Bessaoud, O. (2020). État des lieux de la gestion des ressources en eau et des sols en Algérie. *Revue des Sciences de l'Eau, 33*(2), 109–126. https://doi.org/10.7202/1070644ar

Hamza, N., Ziane, M., &Mehenni, A. (2015). The role of soil types in erosion sensitivity in a Mediterranean context: Case study of Kabylie region. *African Journal of Agricultural Research, 10*(4), 282–290. https://doi.org/10.5897/AJAR2014.8985

Horton, R. E. (1945). Erosional development of streams and their drainage basins: Hydrophysical approach to quantitative morphology. *Geological Society of America Bulletin, 56*(3), 275–370. https://doi.org/10.1130/0016-7606(1945)56[275:EDOSAT]2.0.CO;2

jackmac34, "Algérie, Assekrem – érosion désert", Pixabay, posted 2015

Kouli, M., Soupios, P., &Vallianatos, F. (2020). Assessing erosion-prone areas in semi-arid environments using GIS-based analysis of lithology and topography. *Environmental Earth Sciences, 79*(20), 1–14. https://doi.org/10.1007/s12665-020-09207-w

Kinnell, P. I. A. (2016). Sediment and nutrient transport by overland flow. *HydrologicalProcesses*, 30(12), 2135-2154. DOI: 10.1002/hyp.10747

Lei, X., et al. (2020). Modeling and monitoring hydrological changes in the watershed using TWI and other topographic indices. *Journal of Hydrology*, 582, 124505. DOI: 10.1016/j.jhydrol.2020.124505

Liu, Y., Zhang, X., Fang, H., et al. (2018). Effectiveness of check dams in reducing soil erosion and sediment yield on the Loess Plateau, China. *Hydrology and Earth System Sciences*, 22, 5981–5993.https://doi.org/10.5194/hess-22-5981-2018

Martinez-Carreras, N., et al.(2020). Revisiting the topographic wetness index (TWI): Its application in hydrological models for soil erosion studies. *Hydrological Sciences Journal*, 65(6), 881-895. DOI: 10.1080/02626667.2020.1797921

Moore, I. D., Grayson, R. B., & Ladson, A. R. (1991). *Digital terrain modelling: A review of hydrological, geomorphological, and biological applications*. Hydrological Processes, 5(1), 3–30. https://doi.org/10.1002/hyp.3360050103

Mansouri, H., Boutaleb, S., &Bensaid, A. (2021). Enhancing erosion prediction models through integration of high-resolution soil data: Application to Algerian watersheds. *Geocarto International, 36*(12), 1356–1372. https://doi.org/10.1080/10106049.2019.1668223

Mitasova, H., Mitas, L., Brown, W. M., Gerdes, D. P., Kosinovsky, I., & Baker, T. (2013). Modeling erosion and sediment transport with GIS-based tools. *Environmental Modelling & Software, 30*, 38–49. https://doi.org/10.1016/j.envsoft.2011.05.001

Moore, I. D., Grayson, R. B., & Ladson, A. R. (1991). Digital terrain modelling: A review of hydrological, geomorphological, and biological applications. *Hydrological Processes, 5*(1), 3–30. https://doi.org/10.1002/hyp.3360050103

Mansouri, H., Boutaleb, S., &Bensaid, A. (2021). Enhancing erosion prediction models through integration of high-resolution soil data: Application to Algerian watersheds. *Geocarto International, 36*(12), 1356–1372. https://doi.org/10.1080/10106049.2019.1668223

Mitasova, H., Mitas, L., Brown, W. M., Gerdes, D. P., Kosinovsky, I., & Baker, T. (2013). Modeling erosion and sediment transport with GIS-based tools. *Environmental Modelling & Software, 30*, 38–49. https://doi.org/10.1016/j.envsoft.2011.05.001

Moore, I. D., Grayson, R. B., & Ladson, A. R. (1991). Digital terrain modelling: A review of hydrological, geomorphological, and biological applications. *Hydrological Processes, 5*(1), 3–30. https://doi.org/10.1002/hyp.3360050103

Montgomery, D. R., & Dietrich, W. E. (1992). Channel initiation and the problem of landscape scale. *Science, 255*(5046), 826–830. https://doi.org/10.1126/science.255.5046.826

Morgan, R.P.C. (2005). *Soil Erosion and Conservation* (3rd ed.). Wiley-Blackwell. https://onlinelibrary.wiley.com/doi/book/10.1002/0470854617

Nyssen, J., Poesen, J., Veyret-Picot, M., et al. (2004). Collision of historical land use and soil-conservation structures in Tigray, Ethiopia. *Catena*, 58, 151–165. https://doi.org/10.1016/j.catena.2004.05.001

Nearing, M.A., Pruski, F.F., & O'Neal, M.R. (2017). Projected climate change effects on soil erosion by water. *Climatic Change*, 57, 335–349.https://doi.org/10.1023/B:CLIM.0000024698.56016.4c

Nouiri, M., Tabet-Aoul, A., &Benouahi, A. (2015). Seasonal soil sealing and its impact on runoff in semi-arid Algerian watersheds. *Catena, 135*, 176–185. https://doi.org/10.1016/j.catena.2015.07.012

Nouiri, I., Hadjigeorgiou, J., &Laouar, R. (2015). Soil degradation under arid climatic stress: The case of Algerian plateaus. *CATENA, 135*, 240–250. https://doi.org/10.1016/j.catena.2015.07.012

Nouiri, I., Hadjigeorgiou, J., &Laouar, R. (2015). Soil degradation under arid climatic stress: The case of Algerian plateaus. *CATENA, 135*, 240–250. https://doi.org/10.1016/j.catena.2015.07.012

Panagos, P., Borrelli, P., Meusburger, K., Alewell, C., Lugato, E., &Montanarella, L. (2015). Estimating the soil erosion cover-management factor at the European scale. *Land Use Policy, 48*, 38–50. https://doi.org/10.1016/j.landusepol.2015.05.021

Panagos, P., Borrelli, P., Meusburger, K., Alewell, C., Lugato, E., &Montanarella, L. (2015). Estimating the soil erosion cover-management factor at the European scale. *Land Use Policy, 48*, 38–50. https://doi.org/10.1016/j.landusepol.2015.05.021

Pike, R. J., & Wilson, S. E. (1971). Elevation-relief ratio, hypsometric integral, and geomorphic area-altitude analysis. *Geological Society of America Bulletin, 82*(4), 1079–1084. https://doi.org/10.1130/0016-7606(1971)82[1079:ERHIAA]2.0.CO;2

Prasuhn, V., Liniger, H., & Schmidt, H. (2020). Terracing and its impacts on soil and water conservation in Mediterranean environments. *Land Degradation & Development*, 31, 1340–1352.https://doi.org/10.1002/ldr.3514

Renard, K. G., Foster, G. R., Weesies, G. A., McCool, D. K., & Yoder, D. C. (1997). *Predicting soil erosion by water: A guide to conservation planning with the Revised Universal Soil Loss Equation (RUSLE)* (Agricultural Handbook No. 703). USDA.

Remini, B., Achour, B., & Dehane, D. (2015). Impact of sediment transport of the Chellif River on silting of the Boughezoul reservoir (Algeria). Journal of Water and Land Development, 24(1), 3–10. https://jwld.pl/files/Remini-et-al.pdf

Riley, S. J., DeGloria, S. D., & Elliot, R. (1999). A terrain ruggedness index that quantifies topographic heterogeneity. *Intermountain Journal of Sciences, 5*(1–4), 23–27.

Renard, K. G., Foster, G. R., Weesies, G. A., McCool, D. K., & Yoder, D. C. (1997). *Predicting soil erosion by water: A guide to conservation planning with the Revised Universal Soil Loss Equation (RUSLE)* (Agricultural Handbook No. 703). USDA.

Remini, B., Bensafia, D., &Nasroun, T. (2015). Impact of sediment transport of the Chellif River on silting of the Boughezoul reservoir (Algeria). *Journal of Water and Land Development, 24*(1), 35–40. https://doi.org/10.1515/jwld-2015-0005

Renard, K. G., Foster, G. R., Weesies, G. A., McCool, D. K., & Yoder, D. C. (1997). *Predicting soil erosion by water: A guide to conservation planning with the Revised Universal Soil Loss Equation (RUSLE)*. USDA Agriculture Handbook No. 703.

Renard, K.G., Foster, G.R., Weesies, G.A., McCool, D.K., & Yoder, D.C. (1997). *Predicting Soil Erosion by Water: A Guide to Conservation Planning with the RUSLE*. USDA Agriculture Handbook 703.https://www.ars.usda.gov/arsuserfiles/50201000/rusle/ah_703.pdf

Riley, S. J., DeGloria, S. D., & Elliot, R. (1999). A terrain ruggedness index that quantifies topographic heterogeneity. *Intermountain Journal of Sciences, 5*(1–4), 23–27.

Sahnoune, M., Bouzidi, H., & Kalla, M. (2018). Evaluation of the impact of agricultural and grazing practices on erosion sensitivity in semi-arid environments. *Arabian Journal of Geosciences, 11*(9), 212. https://doi.org/10.1007/s12517-018-3553-6

Sahnoune, M., Bouzidi, H., & Kalla, M. (2018). Evaluation of the impact of agricultural and grazing practices on erosion sensitivity in semi-arid environments. *Arabian Journal of Geosciences, 11*(9), 212. https://doi.org/10.1007/s12517-018-3553-6

Sahnoune, M., Saidi, M., &Toumi, L. (2018). Assessing the impact of land degradation due to overgrazing in semi-arid rangelands of Algeria. *Journal of Arid Land Studies, 28*(1), 17–25.

Strahler, A. N. (1957). Quantitative analysis of watershed geomorphology. *Transactions of the American Geophysical Union, 38*(6), 913–920. https://doi.org/10.1029/TR038i006p00913

Shang, Y., et al. (2021). Evaluation of sediment deposition in a semi-arid catchment using the SPI and SDI models. *Catena*, 196, 104890. DOI: 10.1016/j.catena.2020.104890

Schulte-Moore, L., Liebman, M., & Tyndall, J. (2012). Sediment removal by prairie filter strips in row-cropped watersheds. *Journal of Environmental Quality*, 41, 1531–1539. https://doi.org/10.2134/jeq2011.0473

Shrestha, B., Regmi, A.D., & Thapa, B.B. (2020). Bioengineering techniques for slope stabilization and erosion control: A review. *Ecological Engineering*, 158, 106053. https://doi.org/10.1016/j.ecoleng.2020.106053

Tadesse, T., Legesse, B., &Debele, B. (2022). Review on soil erosion modeling in Ethiopia using RUSLE and GIS. *Environmental Systems Research, 11*(1), 1–16. https://link.springer.com/article/10.1007/s43621-025-01037-8

Van Oost, K., Govers, G., De Albán, M., Quine, T. A., &Heckrath, G. (2009). The impact of agricultural soil erosion on the global carbon cycle. *Nature Geoscience, 2*(8), 553–558. https://www.nature.com/articles/ngeo395

Vente, J., Vercruysse, K., Baartman, J. E. M., &Vanmaercke, M. (2023). Integrating sediment connectivity into soil erosion modeling: A case study from Mediterranean catchments. *Frontiers in Environmental Science, 11*, 1103251. https://doi.org/10.3389/fenvs.2023.1103251

Vanoni, V. A. (Ed.). (1975). *Sedimentation engineering*. ASCE Manual No. 54. American Society of Civil Engineers.

Wilson, J. P., & Gallant, J. C. (2000). *Terrain analysis: Principles and applications*. John Wiley & Sons.

Williams, M.R., & King, K.W. (2014). The effectiveness of vegetative filter strips to reduce nutrient and sediment runoff. *Journal of Environmental Quality*, 43(1), 173–181. https://doi.org/10.2134/jeq2012.0173

Yang, G., et al. (2021). Drainage density and its effect on runoff in arid regions. *EnvironmentalEarth Sciences*, 80(3), 92. DOI: 10.1007/s12665-021-09351-w

Zhang, G. H., Liu, B. Y., & Nearing, M. A. (2010). Sediment delivery ratio in the Chinese Loess Plateau: Spatial variability and controlling factors. *HydrologicalProcesses, 24*(17), 2263–2271. https://doi.org/10.1002/hyp.7648

Zhang, X., & Liu, Y. (2020). Spatial analysis of drainage density and its relationship with land use in arid regions. *Hydrology and Earth System Sciences*, 24(12), 4185-4199. DOI: 10.5194/hess-24-4185-2020

Zhuang, Q., et al. (2021). Advances in hydrological modeling for soil erosion assessment in mountainous areas. *Soil and Tillage Research*, 208, 104846. DOI: 10.1016/j.still.2020.104846

Zhang, W., Li, H., & Yang, X. (2023). A dynamic sediment delivery ratio model based on slope connectivity and rainfall thresholds. *Frontiers in Environmental Science, 12*, 1341868. https://www.frontiersin.org/articles/10.3389/fenvs.2024.1341868/full